Rostro-caudal Connectional Heterogeneity of the Dorsal Part of the Macaque Prefrontal Area 46

Rostro-caudal connectional heterogeneity of the dorsal part of the macaque prefrontal area 46.

Elena Borra[1], Carolina Giulia Ferroni[1], Marzio Gerbella[2], Valentina Giorgetti[1], Chiara Mangiaracina[1], Stefano Rozzi[1], Giuseppe Luppino[1].

[1] *Department of Medicine and Surgery, Neuroscience Unit, University of Parma, Parma, Italy*
[2] *Istituto Italiano di Tecnologia (IIT), Center for Biomolecular Nanotechnologies, Lecce, Italy*

Abbreviated title: Connectional heterogeneity of the macaque area 46d

Corresponding author: Prof. Elena Borra,

Dipartimento di Medicina e Chirurgia, Sezione di Neuroscienze

Università di Parma, Via Volturno 39, I-43125 Parma, Italy.

Phone: +390521903879

Fax: +390521903900

E mail: elena.borra@unipr.it

ABSTRACT

Based on neural tracer injections we found evidence for three connectionally distinct sectors of the dorsal part of the macaque prefrontal area 46 (46d), located at different rostro-caudal levels. Specifically, a rostral sector displayed an almost exclusive and extensive intraprefrontal connectivity and extraprefrontal connections limited to superior temporal areas and the caudal cingulate area 31. Conversely, both a middle and a caudal sector were characterized by robust, topographically organized connections with parietal and frontal sensorimotor areas. Both these sectors shared connections with caudal and medial superior parietal areas (V6A and PGm) where visuospatial information is combined with gaze- and arm-related signals for visuomotor control of arm reaching and/or eye movements. However, the caudal sector was preferentially connected to parietal and frontal oculomotor areas, whereas the middle one was preferentially connected to skeletomotor, mostly arm-related, parietal and premotor areas. The present study provides evidence for a rostro-caudal organization of area 46d similar to that described for the ventrolateral prefrontal cortex, in which more caudal areas are relatively more directly involved in controlling different aspects of motor behavior and more rostral areas are most likely involved in higher order, possibly more abstract, cognitive functions.

Keywords: executive functions; motor control; visuospatial processing; superior parietal lobule; dorsal premotor cortex

INTRODUCTION

Architectonic area 46 of the macaque prefrontal cortex, as originally defined by Walker (1940), is a functionally and connectionally heterogeneous region extending over almost the entire rostro-caudal extent of the principal sulcus (PS) and the immediately adjacent convexity cortex and involved in several aspects of executive control of behavior (see, e.g., Tanji and Hoshi 2008). Recent systematic assessment of the connectivity of the ventral part of area 46 (46v) has provided evidence for connectionally different sectors, located at different rostro-caudal levels (Gerbella et al. 2013). The rostral half of area 46v (46vr) is connected mostly with other prefrontal areas and the inferotemporal cortex, whereas the caudal half with parietal and frontal sensorimotor areas. The connections of the caudal half of area 46v (46vc) are topographically organized: the more caudal part is primarily connected with inferior parietal and prearcuate oculomotor areas, whereas the more rostral part with inferior parietal and ventral premotor hand- and mouth-related areas. These data, together with data on the connectivity of the ventrally adjacent areas 45 and 12r (Gerbella et al. 2010; Borra et al. 2011), suggested a general rostro-caudal functional organization of the macaque ventrolateral prefrontal (VLPF) cortex, in which the caudal part is involved in oculomotor (more caudally) and in skeletomotor (more rostrally) control and the rostral part is involved in higher order integrative aspects of executive functions.

The connectivity of the dorsal part of area 46 (46d) has not been yet systematically investigated. Relevant rostro-caudal connectional differences within this area have been observed by Saleem et al. (2014), but not by Petrides and Pandya (1999), based on relatively few tracer injections. Moreover, indirect evidence showed that posterior parietal and premotor connections of area 46d involve the caudal but not the rostral part of this area (e.g., Cavada and Goldman-Rakic 1989; Andersen et al. 1990; Luppino et al. 1993, 2003; Rozzi et al. 2006; Passarelli et al. 2017), suggesting connectional heterogeneity of this area and similarities with the connectional organization of area 46v.

In the present study, to obtain a more comprehensive picture of the possible topographic organization of the cortical connectivity of area 46d and to assess whether the general organizational principles described for the VLPF also apply to this area, we injected neural tracers at different rostro-caudal levels of area 46d. Preliminary data have been presented in an abstract form (Borra et al. 2014; Luppino et al. 2014).

METHODS

Subjects, surgical procedures, and selection of the injection sites

The experiments were carried out in 5 *Macaca fascicularis* (Cases 23, 57, 58, 60, and 64), in which retrograde and retro-anterograde neural tracers were injected at different rostro-caudal levels of area 46d and in the caudally adjacent area 8r (Table 1). Animal handling as well as surgical and experimental procedures complied with the European law on the humane care and use of laboratory animals (directives 86/609/EEC, 2003/65/CE, and 2010/63/EU) and Italian laws in force regarding the care and use of laboratory animals (D.L. 116/92 and 26/2014), and were periodically approved by the Veterinarian Animal Care and Use Committee of the University of Parma and authorized by the Italian Ministry of Health.

Under general anesthesia (Zoletil®, initial dose: 20mg/kg, i.m.; supplemental: 5–7 mg/kg/h, i.m., or Ketamine, 5 mg/kg i.m. and Medetomidine, 0.08–0.1 mg/kg i.m.) and aseptic conditions, each animal was placed in a stereotaxic apparatus and an incision was made in the scalp. The skull was trephined to remove the bone overlying the target region and the dura was opened to expose the PS and the dorsally adjacent convexity cortex. The choice of the injection sites was based on identified anatomical landmarks, i.e., the superior arcuate sulcus and the PS , and on estimations of the average location of the cytoarchitectonic border of area 46d with the caudally adjacent area 8r (Gerbella et al. 2007). As in Saleem et al. (2014), area 46d was considered to extend along the dorsal bank of the PS and on the immediately adjacent convexity cortex, except for the caudal and rostral end of the sulcus, located within areas 8r and 10, respectively (Fig. 1A). After the tracer injections were placed, the dural flap was sutured, the bone was replaced, and the superficial tissues were sutured in layers. During surgery, hydration was maintained with saline, and temperature using a heating pad. Heart rate, blood pressure, respiratory depth, and body temperature were continuously monitored. Upon recovery from anesthesia, the animals were returned to their home cages and closely monitored. Dexamethasone and prophylactic broad-spectrum antibiotics were

administered pre- and postoperatively. Furthermore, analgesics were administered intra- and postoperatively.

Tracer injections and histological procedures

Once the appropriate site was chosen, the neural tracers Fast Blue (FB, 3% in distilled water, Dr Illing Plastics GmbH, Breuberg, Germany), Diamidino Yellow (DY, 2% in 0.2 M phosphate buffer at pH 7.2, Dr Illing Plastics), Cholera Toxin B subunit, conjugated with Alexa 488 (CTB green, CTBg) or Alexa 594 (CTB red, CTBr; 1% in 0.01 M phosphate-buffered saline at pH 7.4, Molecular Probes, Thermo Fisher Scientific, Waltham, MA, USA), wheat germ agglutinin (WGA; 4% in distilled water, Vector Laboratories, Burlingame, CA), and dextran conjugated with tetramethylrhodamine (Fluoro-Ruby, FR, 10000 MW, 10% 0.1 M phosphate buffer, pH 7.4; Invitrogen) or with lucifer yellow (Lucifer Yellow Dextran, LYD, 10000 MW, 10% 0.1 M phosphate buffer, pH 7.4; Invitrogen, Thermo Fisher Scientific) were slowly pressure-injected through a glass micropipette (tip diameter: 50-100 µm) attached to a 1- or 5-µl Hamilton microsyringe (Reno, NV). Table 1 summarizes the locations of the injections, the injected tracers, and their amounts.

After appropriate survival periods following the injections (28 days for FR and LYD, 12-14 days for FB, DY and CTB conjugates, 48 hours for WGA), each animal was deeply anesthetized with an overdose of sodium thiopental and perfused consecutively with saline, 3.5% formaldehyde, and 5% glycerol, prepared in 0.1 M phosphate buffer, pH 7.4, through the left cardiac ventricle. Each brain was then blocked coronally on a stereotaxic apparatus, removed from the skull, photographed, and placed in 10% buffered glycerol for 3 days and 20% buffered glycerol for 4 days. Finally, each brain was cut frozen into coronal sections of 60-µm thickness. In all cases in which FB, DY and CTB conjugates were injected, a 1-in-5 series was mounted, air-dried, and quickly coverslipped for fluorescence microscopy. In all cases, an additional injection of the the axonal tracer biotinylated dextran-amine (BDA) was placed in a different part of the cortex. We visualized both BDA and the FR, LYD, and, in Case 64l, CTBg in a 1-in-5 series using the double-

labeling protocol described in detail in Gerbella et al. (2010, 2016). In Case 64l, this protocol was adopted to visualize axon terminals anterogradely labeled with CTBg, which is otherwise difficult to detect with fluorescence microscopy. Briefly, the sections were first processed to visualize BDA, i.e., incubated overnight in the ABC solution (Vectastain ABC kit, PK-4000, Vector Laboratories) and then BDA was stained brown using 3,3'-diaminobenzidine (DAB, Sigma-Aldrich, St. Louis, MO). Then, the sections were incubated overnight in avidin-biotin blocking reagent (SP-2001, Vector Laboratories), for 72 h at 4°C in a primary antibody solution of rabbit anti-FR, or rabbit anti-LY (1:3000; Invitrogen), or rabbit anti-Alexa 488 (1:15000, Thermo Fisher Scientific) in 0.5% Triton, 5% normal goat serum in PBS, and 1 h in biotinylated secondary antibody (1:200, Vector Laboratories) in 0.3% Triton, 5% normal goat serum in PBS. Finally, FR, LYD, and CTBg labeling was visualized using the Vectastain ABC kit and the Vector SG peroxidase substrate kit (SK-4700, Vector Laboratories) as a chromogen. With this procedure, BDA labeling was stained brown and the FR, LYD, or CTBg labeling was stained blue in the same tissue sections.

In all cases, a 1-in-5 series was stained with the Nissl method (0.1% thionin in 0.1 M acetate buffer, pH 3.7).

Data analysis

Injection sites and distribution of retrogradely labeled neurons.

The criteria used for defining the injection sites and identifying FB, DY, CTB conjugates, WGA, FR, and LYD labeling have been described in earlier studies (Luppino et al. 2001, 2003; Rozzi et al. 2006; Gerbella et al. 2010, 2011). All the injection sites used in this study were completely restricted to the cortical grey matter, in some cases involving the entire cortical thickness, in other mostly layers III-V. Injection sites were attributed to area 46d or to area 8r based on analysis of adjacent Nissl-stained sections and localized on a 2-dimensional (2D) reconstruction of the injected hemisphere.

Furthermore, to estimate the antero-posterior (AP) position of the injection sites within area 46d, in each case we measured their distance from the architectonic border of area 8r along the AP

stereotaxic plane (Table 1). As we found that the total length of the PS in all cases of injection in 46d (all of them *Macaca fascicularis*) was quite constant across different cases (13.8 mm ±1.0), the AP level of each injection site was then reported on a template hemisphere (Case 23l), in order to obtain a comparative view of their distribution within area 46d (Fig. 1A).

The distribution of retrograde (for all tracer injections) and anterograde (for injections of FR, LYD and CTBg in Case 64l) labeling was analyzed in sections every 300 µm and plotted in sections every 600 µm, together with the outer and inner cortical borders, using a computer-based charting system. The distribution of the labeling in the superior temporal sulcus (STS) was visualized in 2D reconstructions obtained using the same software, as follows (for more details, see Matelli et al. 1998). In each plotted section, the cortical region within the STS was unfolded at the level of a virtual line running approximately along the border between layers III and IV. The unfolded sections were then aligned to correspond with the fundus and the middle of the floor and the labeling was distributed along the space between the two consecutive plotted sections (600 µm). Data from individual sections were also imported into the 3-dimensional (3D) reconstruction software (Demelio et al., 2001) providing volumetric reconstructions of the monkey brain, including connectional and architectonic data.

Areal attribution of the labeling.

The criteria and maps adopted for the areal attribution of the labeling were similar to those adopted in previous studies (Rozzi et al. 2006; Borra et al. 2008; Gerbella et al. 2010, 2011; see Supplementary Fig. 1). In the frontal lobe, prefrontal areas were defined according to cyto- and chemo-architectonic criteria described in Carmichael and Price (1994), Gerbella et al. (2007), and Saleem et al. (2014). Area 46v was subdivided into a rostral and a caudal part based on connectional data described in Gerbella et al. (2013). Furthermore, similarly to Saleem et al. (2008, 2014) based on the labeling distribution, a fundal sector was defined in the PS (fundal 46, 46f). Agranular frontal and cingulate areas and opercular frontal areas were defined according to cyto- and chemo-architectonic criteria described in Matelli et al. (1991, 1985) and Belmalih et al. (2009).

The temporal labeling in the STS cortex was attributed based on the electrophysiological and architectonic map proposed by Boussaoud et al. (1990) and guided by the atlas of Saleem and Logothetis (2012) and the labeling in the superior temporal gyrus (STG) and auditory belt cortex based on the architectonic, functional and connectional map described by Kaas and Hackett (2000; see also Saleem et al. 2008) . In the inferior parietal lobule (IPL), the gyral convexity areas were defined according to cyto- and chemo-architectonic criteria described in Gregoriou et al.(2006) and those of the lateral bank of the intraparietal sulcus based on connectional criteria described in Borra et al.(2008). The medial parietal cortex was defined according to architectonic criteria described in Pandya and Seltzer (1982) and Luppino et al. (2005). Finally, for the caudal cingulate cortex we adopted the cytoachitectonic map proposed in Morecraft et al. (2004).

Quantitative analysis and laminar distribution of the labeling.

In all the retrograde tracer injection cases, except for FR and LYD, we counted the number of labeled neurons plotted in the ipsilateral hemisphere, beyond the limits of the injected area, in sections at every 600 µm interval. Cortical afferents to area 46d were then expressed in terms of the percentage of labeled neurons found in a given cortical subdivision, with respect to the overall labeling found for each tracer injection. FR and LYD injections were excluded from this analysis because of a general paucity of the retrograde transport with respect to the anterograde one and of a dense, nonspecific staining surrounding the injection site, often observed in our immunostained material (see Gerbella et al., 2010), which extended into the adjacent area 8B or 9 and prevented accurate plotting of the retrograde labeling.

Furthermore, to obtain information about the organization of the laminar patterns of the observed connections, the labeling attributed to a given area and reliably observed across different sections and cases was analyzed in sections at every 300 µm in terms of the following: 1) laminar distribution of the anterogradely labeled terminals (for FR, LYD and Case 64l CTBg injections) and 2) amount of retrogradely labeled neurons located in the superficial (II-III) versus deep (V-VI) layers (s/d ratio).

RESULTS

Area 46d, as defined in the present study, occupies almost the entire extent of the dorsal bank of the PS, extending for about 2-3 mm on the dorsally adjacent convexity cortex. In Nissl-stained material, this area shows a cell-dense layer III with an evident size gradient, a well-developed and cell-dense layer IV, and a layer V densely populated by small pyramids (Fig. 2, B, C, and G). Caudally, at the level of the tip of the PS, area 46d borders area 8r, characterized by a relatively small overall thickness, a dense and homogeneous relatively thin layer III, a layer IV thin and difficult to demarcate, and a layer V populated by densely packed small pyramids (Fig. 2, A and E). Dorsally, the caudal part of area 46d borders a cytoarchitectonic field, similar to area 8r, but characterized by larger layer V pyramids (Fig. 2, B and F). This field, designated as area 8A, occupies the rostralmost part of the prearcuate bank and extends on the prearcuate convexity cortex rostral to area 8r (Fig. 1A). More rostrally, the caudal part of area 46d borders area 8B, a further subdivision of area 8 characterized by a faint layer IV and by layers III and V pyramids smaller than in area 8A (see also, Petrides and Pandya, 1999). Further rostrally, area 46d borders area 9, which displays a layer III containing small- to medium-sized pyramids, more darkly stained and large in its deeper part, a narrow, but well-discernible layer IV, and a layer V containing darkly stained, loosely arranged relatively small pyramids (Fig, 2, C and H). Finally, area 46d borders rostrally, in the proximity of the frontal pole, area 10, characterized by a dense layer IV and by vertical and horizontal cross striations of cells in layer III and V.

The injection sites in area 46d used in the present study were all entirely located within its architectonic limits at different rostro-caudal levels, involving mainly the shoulder and the upper part of the dorsal bank of the PS (Fig. 1). As will be shown later, the results provided evidence for different connectivity patterns observed after the injections were placed in the caudal (up to about 3 mm from the 8r/46d border), the middle (from about 3 to about 6 mm rostral to the 8r/46d border), and the rostral (from about 7 to about 11 mm rostral to the 8r/46d border) part of area 46d (Fig. 1A). Accordingly, the results will be presented in three separate sections. A further section will describe

the results from two additional cases of tracer injection placed in the dorsal part of area 8r to compare the connections of this area with those of the caudal 46d.

Connections of the caudal part of area 46d

Three tracer injections (Cases 23l DY, 58r FB, and 60r FR) were placed in the caudal part of area 46d (Fig. 1). The results from these cases will be described based on the distribution of the retrograde labeling observed in Cases 23l DY and 58r FB shown in Figure 3 and in Table 2. In spite of some differences observed across the different cases, one major common feature was a robust connectivity with frontal and parietal oculomotor-related areas.

In the prefrontal cortex, most of the labeling was located in the caudal prefrontal areas 8r and 8A, dorsal part of area 8-FEF (frontal eye field), and area 8B (Fig. 3, sections a-f). Dense labeling was also observed in fundal 46. Less dense connections were observed with areas 9 and 46vc (Fig. 3, sections a and e). In Case 58r FB additional, relatively weak labeling was observed in areas 46vr, 45B, and 45A (Fig. 3, sections a, d and e). Outside the prefrontal cortex, rich labeling was found in the agranular frontal area F7, especially in the dorsal and rostral part where the supplementary eye field (SEF) is located (Fig. 3, sections e and f). In the intraparietal sulcus, relatively rich labeling involved area LIP in all the cases, extending in Case 58r FB also to the adjacent inferior parietal area Opt (Fig. 3, sections k-n). In the medial parietal cortex, there were dense connections with area V6A, especially in Case 58r FB, mostly in the ventral sector (V6Av), and with area PGm (Fig. 3 sections j-n). In the cingulate cortex, relatively rich labeling involved the caudal cingulate cortex, including areas 23a and 23b on the cingulate gyrus and areas 31 and 23 in the retrosplenial cortex (Fig. 3 sections g and i-l), while in the rostral cingulate cortex weak labeling involved different subdivisions of area 24. Finally, in Case 58r FB labeling was found also in the caudal sector of the superior temporal polysensory (STP) area (Figure 3 sections g, h).

Connections of the middle part of area 46d

Five tracer injections (Cases 57r WGA, 60l FB, 60r LYD, 60l CTBr, and 64l FR) were placed in the middle part of area 46d (Fig. 1). All these cases were characterized by rich connectivity with

dorsal premotor and caudal and medial parietal arm-related areas, involved in controlling reaching and reaching-grasping movements. However, some qualitative and/or quantitative connectional differences were observed depending on the rostro-caudal position of the injection site. Accordingly, the connectivity of this sector will be described based on the distribution of the retrograde labeling observed in Cases 57r WGA and 60l FB, in which the injection site was placed more caudally, and in Case 60l CTBr, in which the injection site was placed more rostrally (Figs. 4 and 5 and Table 2).

In the prefrontal cortex, the labeling involved areas 9, 8B, 8r, 46vc, fundal 46, and 46vr. In Cases 57r WGA and 60l FB, the labeling was denser in areas 46vc and fundal 46, whereas in Case 60l CTBr it was denser in areas 9, 8B, and 46vr and extended in area 10 (Figs. 4 and 5, sections a-d and a'-d'). Additional labeling, especially in Case 60l FB, was located in areas 8A, 8-FEF, 45B, and 12l (Table 2). Finally, clusters of labeled cells were observed in the orbitofrontal areas 11 and 13 (Figs. 4 and 5, sections a and a' and d'). In the agranular frontal cortex (Figs. 4 and 5, sections d-f and d' and e'), very dense labeling extensively involved area F7, especially that part located outside the SEF (area F7 non-SEF) and dense labeling was located in area F6. In Cases 57r WGA and 60l FB there was rich labeling in area F2 and weaker labeling in areas F5 and GrFO (Table 2), whereas in Case 60l CTBr there was relatively weak labeling only in area F2 (Table 2). In the parietal cortex, dense labeling was located in area PGm (Figs. 4 and 5, sections i-k and h' and i'). After the more caudal injections, there was also labeling involving the caudal part of the IPL, mostly area PG, and the caudal part of the superior parietal lobule, mostly in the dorsal part of area V6A (V6Ad; Figs. 4 A and B and 5 sections h-j, l and m). In the cingulate cortex, in all cases there was labeling involving mostly rostral and caudal subdivisions of the cingulate gyrus (areas 24a, 24b, 23a, and 23b) and the retrosplenial area 31 (Figs. 4 and 5, sections c, e, g, b',c' and e'-g').

Connections of the rostral part of area 46d

Three tracer injections (Cases 64r DY and 64l LYD and CTBg) were placed in the rostral part of area 46d (Fig. 1). The results from these cases will be described based on the distribution of the

retrograde labeling observed in Cases 64r DY and 64l CTBg, shown in Figures 6 and 7 and in Table 2. The connectivity patterns observed in all the cases were quite similar and characterized by a very strong intraprefrontal connectivity and an extraprefrontal connectivity virtually all confined to superior temporal and caudal cingulate areas.

In the prefrontal cortex (Figs. 6 and 7, sections a-h), very dense labeling was located in the polar and rostral prefrontal areas 10, 9, and 46vr and, more caudally, in fundal 46 and in areas 8B, 8r and 8-FEF. Relatively dense labeling was observed also in the VLPF with some differences across cases: whereas cluster of labeled cells were located in all cases in area 12l, in Case 64l CTBg (Fig. 8J, but also in Case 64l LYD) the labeling involved also area 45A. Finally, in Case 64l CTBg some labeling was located in orbitofrontal areas 11 and 13. Outside the prefrontal cortex, relatively rich labeling involved the superior temporal cortex in two adjacent cortical sectors: the upper bank of the STS, in the location of area STP, especially in the middle and caudal part, and the adjacent convexity cortex of the superior temporal gyrus in the location of the rostral and caudal auditory parabelt cortex (Figs. 6 and 7, sections i-m). Furthermore, relatively dense labeling was located in the retrosplenial cortex, in areas 23 and 31 (Figs. 6 and 7, sections l and m).

Laminar distribution of the labeling

The laminar distribution of both the retrograde and the anterograde labeling in the areas connected to the various sectors of area 46d fell within two main patterns shown in Figure 8. The retrograde labeling was considerably denser in the superficial layers (s/d ratio >2) in all parietal, temporal, cingulate and caudal VLPF areas (e.g., Fig. 8 B and C), whereas it tended to be more equally distributed in the superficial and deep layers in area 46v, 9, and 10. This last pattern was also observed in the premotor areas in all cases except for the rostral injection in the middle part of area 46d (Case 60l CTBr) in which the retrograde labeling in area F7 tended to be richer in the superficial layers (e.g., Fig. 8 F and G). The anterograde labeling showed a columnar organization encompassing all cortical layers in the majority of the connected areas (Fig. 8, A, D, H, I), whereas it was located primarily in layers I-III in areas 45A, STP, STG, LIP, and V6A (e.g., Fig 8 E and J).

Connections of the dorsal part of area 8r

Two tracer injections (Cases 58r DY and 60l CTBg) were placed in the dorsal part of area 8r, near the caudal tip of the PS (Fig. 1). The results from Case 60l CTBg are shown in Figure 9 and the quantitative analysis of the two cases is shown in Table 2. The distribution of the retrograde labeling observed in the two cases was similar to that previously described for the ventral part of this area (Gerbella et al., 2010) and different from that observed after the injections were placed in the caudal part of area 46d.

In both cases, most of the labeling was located in the adjacent areas 8-FEF (mostly in the dorsal part) and 46d. The labeling involved less densely also areas 8A, 8B, 45B and fundal 46. Furthermore, relatively dense labeling was observed in the rostral part of area 46d and in area 45A and, in Case 58r DY, in 46vc and 46vr (Fig. 9, sections a-f). Outside the prefrontal cortex, the labeling involved the SEF in the premotor cortex (Fig. 9, section b), the intraparietal area LIP in the parietal cortex (Fig. 9, section h and i), and the caudal part of the STS (caudal area STP, and areas MST and FST; Fig. 9C and section g) in the temporal cortex. Additional labeling in Case 60l CTBg involved the ventral portion of area V4, near the occipito-temporal sulcus (Figure 9 section i), whereas sparse cells were found in ventral area V2 and in the dorsal prelunate area.

In both cases, retrogradely labeled neurons were almost equally distributed in the superficial and deep layers in areas 46d and 8-FEF, whereas they tended to be denser in the superficial layers (s/d ratio >2) in all the other labeled areas.

DISCUSSION

In the present study we describe the fine grained organization of the cortical connectivity of area 46d, based on relatively restricted tracer injections placed at different rostro-caudal levels, along its whole extent. The results, summarized in Figures 10 and 11, provided evidence for three connectionally distinct sectors of this area. A rostral sector (Figs. 10 C and D and 11C) was characterized by connections mostly with other prefrontal areas and extraprefrontal connections with superior temporal areas, whereas a middle and a caudal sector by robust connectivity with parietal and frontal sensorimotor areas (Fig. 10D). The parietal and frontal connections of these two sectors were topographically organized: the middle sector (Figs. 10B and 11B) was preferentially connected to skeletomotor, mostly arm-related, areas, whereas the caudal one (Figs. 10A and 11A) preferentially to oculomotor areas. Furthermore, the present study shows that the dorsal part of area 8r displays connections very similar to those of its ventral part and different from those of the adjacent caudal area 46d, further supporting the notion that area 8r is a cortical entity distinct from both areas 8-FEF and 46.

Cortical connections of area 46d

The results of the present study extend previous observations on the connectivity of area 46d by Petrides and Pandya (1999) and Saleem et al. (2014), based on two and three tracer injections, respectively, placed at different rostro-caudal levels. Petrides and Pandya (1999) did not describe significant differences in the parietal and temporal connectivity of the rostral vs. the caudal part of area 46d (corresponding to areas 46 and 9/46d, respectively, in their nomenclature). This major difference with the results of the present study could be accounted for by the relatively large size of injection sites in the study of Petrides and Pandya (1999), which could have involved more than one of the connectionally different area 46d sectors identified in the present study. However, note that after the more rostral injection of the study of Petrides and Pandya (1999) the parietal labeling was very weak and confined to area Opt, which is in line with the present data. Saleem et al. (2014), in their study focused on the general connectivity of the lateral prefrontal cortex, have placed one

tracer injection very rostrally in area 46d and another one in the middle 46d, which showed different connectivity patterns, very similar to those observed in the present study after the injections were placed in the rostral and the middle area 46d sector, respectively. Interestingly, the connectivity pattern observed after their middle 46d injection was reported as “exceptional”, as it was not seen in any of the other cases of dorsolateral prefrontal (DLPF) injections, and possibly indicative of a distinct field. The present study provides firm evidence for the connectional distinctiveness of this area 46d sector. The present finding showing that the rostral, but not the middle and the caudal 46d is connected to auditory-related temporal areas is in agreement with the study of Romanski et al. (1999) in which these connections were observed after tracer injections in area 46d only when the injection sites involved the rostral part of this area.

Finally, in agreement with Saleem et al. (2014), the present data showed that the fundal area 46 displays extensive connections with the entire extent of area 46d and, as shown by Saleem et al., (2014) with several other ventral and dorsal prefrontal areas. To our knowledge, in all connectional studies of area 46, including the present one, injection sites have involved the shoulder or the upper part of either the dorsal or the ventral bank of the PS and in none of them neural tracers have been purposefully and selectively injected in the fundal part. Accordingly, direct connectional evidence for the distinctiveness of this sector is still lacking.

The distinction between the rostral vs. the middle and the caudal sector of area 46d finds support also from indirect evidence showing that after injections in premotor (F7, F2, and F6/pre-SMA; Luppino et al. 1993, 2003; Marconi et al. 2001; Takahara et al. 2012), caudal superior and medial parietal (V6A and PGm; Leichnetz 2001; Gamberini et al. 2009; Passarelli et al. 2011, 2017) and IPL (Opt, PG, and LIP; Cavada and Goldman-Rakic 1989; Rozzi et al. 2006) areas, the labeling in area 46d was mostly confined to the middle and the caudal part. Furthermore, tracer injections in area STP, especially in its caudal half, showed prefrontal labeling involving the caudal and the rostral, but not the middle, part of area 46d (Seltzer and Pandya 1989; Saleem et al. 2008). Finally,

injections in the auditory parabelt cortex showed labeling in the rostral, but not in the middle and in the caudal sectors of area 46d (Petrides and Pandya 1988; Saleem et al. 2008).

The marked differences in connectivity patterns observed between the rostral 46d sector mostly connected with other prefrontal and with superior temporal areas and the middle and the caudal sectors characterized by robust connectivity with parietal and frontal sensorimotor areas, to some extent recall the rostro-caudal connectional differences observed for VLPF areas 46v and 12r (Borra et al. 2011; Gerbella et al. 2013). Indeed, the rostral part of both areas 46v and 12r is connected mostly with other prefrontal and with temporal (mostly inferotemporal) areas, whereas the caudal part of area 46v (46vc) and the intermediate and the caudal parts of area 12r display robust connectivity with IPL, opercular parietal, ventral premotor, and prearcuate hand/mouth- or eye-related areas. Furthermore, similarly to what is observed for the caudal and the middle 46d sectors, the caudal part of 46vc ("caudal" 46v) and the caudal 12r are preferentially connected to parietal and frontal oculomotor areas, whereas the rostral 46vc ("middle" 46v) and the intermediate area 12r are preferentially connected to parietal and ventral premotor hand- and mouth-related fields. Thus, the present study suggests that some general principles of the organization of the VLPF connectivity apply also to area 46d. Barbas and Mesulam (1985), after very large tracer injections involving both the dorsal and the ventral lips of the principal sulcus, suggested a distinction between a more rostral "limbic" and a more caudal "visuomotor" part of area 46. It is noteworthy that changes in connectivity patterns observed in the present study along the rostro-caudal extent of area 46d appear to be less sharp than those observed in VLPF areas. For example, dorsal premotor area F7 and parietal areas PGm and V6A were found to be connected to both the caudal and the middle area 46d sectors, though projections from F7 and V6A originated mostly from different sectors of these areas, namely F7-SEF and V6Av for caudal 46d sector and F7- non SEF and V6Ad for the middle 46d sector. Furthermore, even after injections in the rostral 46d, some very small clusters of neurons in area F7 in two out of three cases were observed.

Finally, the present study provides further evidence for the connectional distinctiveness of the prearcuate area 8r. Specifically, our tracer injections placed in the dorsal part of this area showed a very high prefrontal connectivity, almost limited to the neighboring areas and to area 45A, a low temporal connectivity, involving caudal STS areas, and a parietal connectivity virtually limited to area LIP. This connectivity pattern distinguishes area 8r from the caudal 46d and from the caudally adjacent dorsal part of area 8-FEF, which is characterized by much more extensive prefrontal and temporal connectivity (Huerta et al. 1987; Stanton et al. 1993, 1995; Schall et al. 1995; Gerbella et al. 2010). Furthermore, the connectional features of the dorsal part of area 8r appear substantially similar to those observed after the tracer injections were placed in its ventral part (Gerbella et al., 2010). However, the dorsal part of area 8r connects with mostly the dorsal part of area 8-FEF, which represents large-amplitude saccades (Bruce et al. 1985), whereas the ventral part of area 8r connects with mostly the ventral part of area 8-FEF, which represents small saccades. This pattern of connectivity suggests a topographic organization for eye movement representations in area 8r.

Functional considerations

The lateral prefrontal cortex is essential for executive functions and consists of several functionally distinct fields specified by different connectivity patterns (e.g., Tanji and Hoshi 2008).

Specifically, area 46d was once considered as part of a larger prefrontal domain involved in working memory for visuospatial information, distinct from a more ventral domain primarily involved in working memory for non-spatial information (Goldman-Rakic 1987; Levy and Goldman-Rakic 2000). However, neural activity in area 46d can be also tuned to both the identity and location of objects (Rao et al. 1997). Other studies have provided evidence for a wider role of this area in controlling higher order aspects of behavior. Specifically, neurons in DLPF cortex including area 46d display activity related to behavioral goals (e.g., Yamagata et al. 2012), task progress (Hasegawa et al. 2004; Ninokura et al. 2004), hierarchical representation of task events (Sigala et al. 2008), retrieval of task-relevant information and integration of different sets of information for action planning (Hoshi and Tanji 2004; see also Tanji and Hoshi 2008) and encode

both cognitive and motor aspects of tasks requiring drawing of geometrical shapes (Averbeck et al., 2003; 2009). Furthermore, it has been suggested that more rostral sectors of areas 46d and 9 are involved in the selection of abstract response strategies for cognitive problems (Genovesio et al. 2005; Tsujimoto et al. 2011) and in the representation of previous and future goals (Genovesio et al. 2006).

The present connectional data are helpful for gaining insight into a possible differential role of distinct parts of area 46d, in controlling different aspects of behavior. The caudal and middle sectors of area 46d share common connections with caudal superior and medial parietal areas (V6A and PGm) and the adjacent area 31, involved in visuospatial information processing and visuomotor control of arm reaching and/or eye movements (Galletti et al. 1996, 1997, 1999, 2003; Olson et al. 1996; Ferraina et al. 1997a, 1997b; Battaglia-Mayer et al. 2000, 2001; Dean and Platt 2006). Interestingly, a recent hierarchical cluster analysis of the macaque parieto-frontal connectivity showed that areas V6A, PGm, and 31 form a cluster distinct from other clusters of superior parietal areas (Caminiti et al. 2017). The present data are in line with the results of this analysis and suggest that connectivity with area 46d is a feature that distinguishes this cluster from the other superior parietal clusters involved in visuo- and/or somato-motor transformations for reaching. Specifically, area V6A, as a whole, hosts saccade-related neurons and reaching, or reaching-grasping neurons (Galletti et al. 1995, 1997; Kutz et al. 2003; Fattori et al. 2010) coding target depth and direction based on arm- and gaze-related signals (Hadjidimitrakis et al. 2014). In V6Av, which is preferentially connected to the caudal area 46d sector, most of the neurons are visually-responsive and are activated by simple static or moving (especially at fast velocity) stimuli, whereas in V6Ad, which is preferentially connected to the middle area 46d sector (Gamberini et al. 2009; present data) visual neurons respond preferentially to complex stimuli and neurons responding to somatosensory stimuli are highly represented (Gamberini et al. 2011). Area PGm hosts neurons combining local and virtual egomotion and whose neural activity is related to navigation in a virtual environment (Sato et al. 2010) and has been considered to be part of a cortical network involved in spatial

navigation (Kravitz et al., 2011). Neurons encoding spatial locations in an allocentric frame of reference, which can be used for navigation as well as for visomotor control, have been found also in the adjacent area 31 (Dean and Platt 2006).

Several connectional features, however, distinguish the caudal from the middle area 46d sectors. Specifically, the caudal sector is directly connected to areas LIP, 8-FEF, and F7-SEF, which are in turn connected with one another and take part to a frontoparietal network for initiating and controlling voluntary eye movements and for orienting attention in space (see, e.g., Thompson and Bichot, 2005; Lynch and Tian 2006). Furthermore, the caudal 46d sector is also connected to area 8r and the caudal 46vc, which, in turn, are connected to areas 8-FEF, F7-SEF, and LIP and are provided with descending projections to oculomotor brainstem structures (Borra et al. 2015). Indeed, this sector and the caudal 46vc have been collectively defined as “prefrontal FEF” by Lynch and Tian (2006). Altogether, these data provide firm anatomical evidence for the involvement of the caudal 46d sector in the frontoparietal oculomotor network. Specifically, this sector appears to be involved in working memory of the location in space of targets of saccades (see Lynch and Tian, 2006) and could interact with area LIP during the performance of an oculomotor delayed response (Chafee et al., 2000). Furthermore, it could contribute to the known role of area 8-FEF in top-down control of spatial attention based on knowledge and goals of the viewer that is crucial for stimulus selection and voluntary orientation of spatial attention (e.g., Thompson and Bichot, 2005; Ibos et al., 2013).

In contrast, the middle area 46d sector is connected with arm-related premotor fields (F7-non SEF, and F2vr), which, as this 46d sector, are connected with areas V6A and PGm (e.g., Matelli et al., 1998, Gamberini et al., 2009). Area F7-non SEF hosts neurons showing eye-and arm-related activity (Fujii et al. 2000) and coding position in space of targets for reaching movements (Vaadia et al. 1986). Area F2vr hosts a mostly distal arm movement representation in which there are visuomotor grasping neurons encoding object features (Raos et al. 2004) and specifying object location relative to the monkey’s peri- or extrapersonal space (Fogassi et al. 1999). It has been

proposed that visuomotor parieto-frontal circuits linking caudal superior parietal with PMd areas could play an important role in relatively fast feed-forward guidance and online monitoring of reach-to-grasp actions (Fattori et al. 2015). The present data provide direct evidence for involvement of the middle area 46d sector in this circuitry. Accordingly, this sector could represent a prefrontal node of a parieto-premotor-prefrontal network involved in visuomotor control of reaching-grasping movements (dorsal reaching–grasping network; see Borra et al. 2017). The present data also showed connections of the middle 46d sector with the hand-related PMv area F5 and the adjacent interconnected area GrFO. Area F5 is a complex of different subdivisions which, altogether, take part to a large scale temporo-parieto-frontal network, involving the "middle" 46v, and playing an important role in generating and controlling purposeful hand actions (lateral grasping network; Borra et al., 2017). This 46d-F5 connection could represent one possible substrate for interactions between the dorsal reaching–grasping network and the lateral grasping network (see Borra et al., 2017). The relatively deep location of the labeling observed in the postarcuate bank can account for the paucity of the labeling observed in area 46d after tracer injections in area F5 (Gerbella et al. 2011). Furthermore, the middle 46d sector is connected with area F6, an arm-related premotor area involved in higher order aspects of motor control (see, e.g., Picard and Strick 2001; Nachev et al. 2008) and connected with parietal and frontal areas of both the dorsal reaching–grasping and the lateral grasping networks. Finally, the middle 46d sector is connected to the IPL area PG, which appears to be involved in space coding based on high-order multisensory integration for guiding arm motor behavior (Rozzi et al. 2008).

Altogether, the present data suggest a general role of the middle and caudal area 46d sectors in executive functions based on different aspects of visuospatial processing and specialized for controlling arm/hand and eye motor behavior, respectively. In the literature to date, there is some evidence that cells representing oculomotor responses tend to be located in the caudal-most part of area 46d (e.g., Boch and Goldberg 1989; Averbeck et al. 2006; Ichihara-Takeda and Funahashi 2007) and there is some indication that the representation of arm or hand movements is located

more rostrally, possibly corresponding to the middle area 46d (Requin et al. 1990). However, a clear functional segregation reflecting the connectional differences observed in the present study remains to be demonstrated.

The present connectional data also showed that the rostral 46d sector is characterized by an almost exclusive intraprefrontal connectivity involving mostly DLPF but also VLPF areas and extraprefrontal connectivity substantially involving superior temporal and caudal cingulate areas. This connectivity pattern, markedly different from that of the middle and the caudal 46d, is in line with data suggesting a role of this sector in higher order aspects of the cognitive control of behavior (Genovesio et al. 2005, 2006; Tsujimoto et al. 2011). Interestingly, the present data showed that this sector is connected to the dorsal part of area 8-FEF, areas 45A and STP, and the auditory parabelt cortex, which in turn are all connected with one another (Huerta et al. 1987; Petrides and Pandya 1988; Seltzer and Pandya 1989; Stanton et al. 1993, 1995; Schall et al. 1995; Gerbella et al. 2010; Saleem et al. 2014). Area STP is involved in the integration of audiovisual communication signals (Barraclough et al. 2005; Chandrasekaran and Ghazanfar 2008; Dahl et al. 2009), and hosts face or body-parts responsive neurons sensitive to the gaze direction, which may be relevant in understanding where the conspecifics are fixating (Mistlin and Perrett 1990; Carey et al. 1997; Jellema et al. 2000). Like area STP, also area 45A, a caudal VLPF area affiliated to the frontal oculomotor system (Gerbella et al. 2010; Borra et al. 2015), is involved in the integration of audiovisual communication signals (Sugihara et al. 2006; Romanski and Averbeck 2009; Diehl and Romanski 2014). Thus, areas STP, 45A and 8-FEF appear to form a superior temporal-frontal network, likely involved in communication behavior and providing the possible neural substrate for the role of gaze position and eye movements in social behavior (Gerbella et al., 2010). Indeed, in monkeys, eye-gaze direction is important in the expression of dominant or submissive social signaling (Tate et al. 2006). Furthermore, during social interactions monkeys fixate predominantly on the eye region of vocalizing conspecifics, which probably contributes to the perception of that individual's social intentions (Ghazanfar et al. 2006). The present data suggest that rostral 46d is a

rostral prefrontal sector that contributes to this “social/oculomotor” network, based on integration of social cues, allocentric visuospatial information originating from the caudal cingulate area 31, and higher order processing of behavioral strategies.

Finally, in a broader context, the present study provides additional evidence for a general rostro-caudal organization of the macaque lateral prefrontal cortex, originally described for the VLPF (Borra et al. 2011; Gerbella et al. 2013) in which more caudal areas are relatively more directly involved in controlling different aspects of motor behavior and more rostral areas are most likely involved in higher order, possibly more abstract, cognitive functions (Fig. 11D). In recent years, neuroimaging studies have provided mounting evidence for rostro-caudal functional gradients in the human prefrontal cortex. Specifically, some authors have proposed that progressively rostral prefrontal areas perform progressively higher levels of cognitive control through processing increasingly abstract representations (Koechlin and Summerfield, 2007; Badre and D’Esposito, 2009). Other authors have pointed to rostro-caudal gradients in relational integration (Wendelken et al., 2008), in processing event sequence knowledge depending on how often the activity is performed in daily life (Krueger et al., 2007), and in the representation of behavioral hierarchies (Botvinick, 2008). It is possible that this general rostrocaudal functional organization of the human prefrontal cortex is based on rostrocaudal connectional gradients similar to those described in the macaque.

FUNDING

The work was supported by Ministero dell'Istruzione, dell'Università e della Ricerca (grant number: PRIN 2010, 2010MEFNF7_005), European Commission Grant Cogsystems FP7–250013, and Interuniversity Attraction Poles (IAP) P7/11.

ACKNOWLEDGEMENTS

The 3D reconstruction software was developed by CRS4, Pula, Cagliari, Italy.

REFERENCES

Andersen RA, Asanuma C, Essick G, Siegel RM. 1990. Corticocortical connections of anatomically and physiologically defined subdivisions within the inferior parietal lobule. J Comp Neurol. 296:65–113.

Averbeck BB, Chafee MV, Crowe DA, Georgopoulos AP. 2003. Neural activity in prefrontal cortex during copying geometrical shapes. I. Single cells encode shape, sequence, and metric parameters. Exp Brain Res. 150:127-141.

Averbeck BB, Crowe DA, Chafee MV, Georgopoulos AP. 2009. Differential contribution of superior parietal and dorsal-lateral prefrontal cortices in copying. Cortex.45:432-441.

Averbeck BB, Sohn JW, Lee D. 2006. Activity in prefrontal cortex during dynamic selection of action sequences. Nat Neurosci. 9:276–282.

Badre D, D'Esposito M. 2009. Is the rostro-caudal axis of the frontal lobe hierarchical?. Nat Rev Neurosci. 10:659-669.

Barbas H, Mesulam M. 1985. Cortical afferent input to the principals region of the rhesus monkey. Neuroscience. 15:619–37.

Barraclough NE, Xiao DK, Baker CI, Oram MW, Perrett DI. 2005. Integration of visual and auditory information by superior temporal sulcus neurons responsive to the sight of actions. J Cogn Neurosci. 17:377–391.

Battaglia-Mayer A, Ferraina S, Genovesio A, Marconi B, Squatrito S, Molinari M, Lacquaniti F, Caminiti R. 2001. Eye-hand coordination during reaching. II. An analysis of the relationships between visuomanual signals in parietal cortex and parieto-frontal association projections. Cereb Cortex. 11:528–544.

Battaglia-Mayer A, Ferraina S, Mitsuda T, Marconi B, Genovesio A, Onorati P, Lacquaniti F, Caminiti R. 2000. Early coding of reaching in the parietooccipital cortex. J Neurophysiol. 83:2374–2391.

Belmalih A, Borra E, Contini M, Gerbella M, Rozzi S, Luppino G. 2009. Multimodal architectonic subdivision of the rostral part (area F5) of the macaque ventral premotor cortex. J Comp Neurol. 512:183-217.

Boch RA, Goldberg ME. 1989. Participation of prefrontal neurons in the preparation of visually guided eye movements in the rhesus monkey. J Neurophysiol. 61:1064–1084.

Borra E, Belmalih A, Calzavara R, Gerbella M, Murata A, Rozzi S, Luppino G. 2008. Cortical connections of the macaque anterior intraparietal (AIP) area. Cereb Cortex. 18:1094–1111.

Borra E, Gerbella M, Giorgetti V, Rozzi S, Luppino G. 2014. Connectional heterogeneity of the macaque dorsal prefrontal area 46 (46d). Washington, DC: Society for Neuroscience, Online. p. Program No 249.12, 2014 Neuroscience Meeting Plann.

Borra E, Gerbella M, Rozzi S, Luppino G. 2011. Anatomical evidence for the involvement of the macaque ventrolateral prefrontal area 12r in controlling goal-directed actions. J Neurosci. 31:12351–12363.

Borra E, Gerbella M, Rozzi S, Luppino G. 2015. Projections from caudal ventrolateral prefrontal areas to brainstem preoculomotor structures and to basal ganglia and cerebellar oculomotor loops in the macaque. Cereb Cortex. 25:748–764.

Borra E, Gerbella M, Rozzi S, Luppino G. 2017. The macaque lateral grasping network: A neural substrate for generating purposeful hand actions. Neurosci Biobehav Rev. 75:65–90.

Botvinick M.M. 2008. Hierarchical models of behavior and prefrontal function. Trends Cogn Sci. 12:201-208

Boussaoud D, Ungerleider LG, Desimone R. 1990. Pathway for motion analysis: cortical connections of the medial superior temporal and fundus of the superior temporal visual areas in the macaque. J Comp Neurol. 296:462–495.

Bruce CJ, Goldberg ME, Bushnell MC, Stanton GB. 1985. Primate frontal eye fields. II. Physiological and anatomical correlates of electrically evoked eye movements. J Neurophysiol. 54:714–734.

Caminiti R, Borra E, Visco-Comandini F, Battaglia-Mayer A, Averbeck BB, Luppino G. 2017. Computational architecture of the parieto-frontal network underlying cognitive-motor control in monkeys. eNeuro. 2017 Feb 27;4(1). pii: ENEURO.0306-16.2017.

Carey DP, Perrett DI, Oram MW. 1997. Recognizing, understanding and reproducing action. In: Boller F,, Grafman J, editors. Handbook of Neuropsychology, vol II. Amsterdam: Elsevier. p. 111–130.

Carmichael ST, Price JL. 1994. Architectonic subdivision of the orbital and medial prefrontal cortex in the macaque monkey. J Comp Neurol. 346:366–402.

Cavada C, Goldman-Rakic PS. 1989. Posterior parietal cortex in rhesus monkey: II. Evidence for segregated corticocortical networks linking sensory and limbic areas with the frontal lobe. J Comp Neurol. 287:422–445.

Chafee MV, Goldman-Rakic PS. 2000. Inactivation of parietal and prefrontal cortex reveals interdependence of neural activity during memory-guided saccades. J Neurophysiol. 83:1550-1566.

Chandrasekaran C, Ghazanfar AA. 2008. Different neural frequency bands integrate faces and voices differently in the superior temporal sulcus. J Neurophysiol. 101:773–788.

Dahl CD, Logothetis NK, Kayser C. 2009. Spatial organization of multisensory responses in temporal association cortex. J Neurosci. 29:11924–11932.

Dean HL, Platt ML. 2006. Allocentric spatial referencing of neuronal activity in macaque posterior cingulate cortex. J Neurosci. 26:1117–1127.

Demelio S, Bettio F, Gobbetti E, Luppino G. 2001. Three-dimensional reconstruction and visualization of the cerebral cortex in primates. In; Ebert D, Favre J, Peikert R, editors. Data Visualization 2001. New York, NY, USA:Springer Verlag. p 147-156

Diehl MM, Romanski LM. 2014. Responses of prefrontal multisensory neurons to mismatching faces and vocalizations. 34:11233–11243.

Fattori P, Breveglieri R, Bosco A, Gamberini M, Galletti C. 2015. Vision for prehension in the

medial parietal cortex. Cereb Cortex. bhv302.

Fattori P, Raos V, Breveglieri R, Bosco A, Marzocchi N, Galletti C. 2010. The dorsomedial pathway is not just for reaching: Grasping neurons in the medial-parieto-occipital cortex of the macaque monkey. J Neurosci. 30:342–349.

Ferraina S, Garasto MR, Battaglia-Mayer A, Ferraresi P, Johnson PB, Lacquaniti F, Caminiti R. 1997a. Visual control of hand-reaching movement: activity in parietal area 7m. Eur J Neurosci. 9:1090–1095.

Ferraina S, Johnson PB, Garasto MR, Battaglia-Mayer A, Ercolani L, Bianchi L, Lacquaniti F, Caminiti R. 1997b. Combination of hand and gaze signals during reaching: activity in parietal area 7 m of the monkey. J Neurophysiol. 77:1034–1038.

Fogassi L, Raos V, Franchi G, Gallese V, Luppino G, Matelli M. 1999. Visual responses in the dorsal premotor area F2 of the macaque monkey. Exp brain Res. 128:194–199.

Fujii N, Mushiake H, Tanji J. 2000. Rostro-caudal distinction of the dorsal premotor area based on oculomotor involvement. J Neurophysiol. 83:1764–1769.

Galletti C, Battaglini PP, Fattori P. 1995. Eye position influence on the parieto-occipital area PO (V6) of the macaque monkey. Eur J Neurosci. 7:2486–2501.

Galletti C, Fattori P, Battaglini PP, Shipp S, Zeki S. 1996. Functional demarcation of a border between areas V6 and V6A in the superior parietal gyrus of the macaque monkey. Eur J Neurosci. 8:30–52.

Galletti C, Fattori P, Kutz DF, Battaglini PP. 1997. Arm movement-related neurons in the visual area V6A of the macaque superior parietal lobule. Eur J Neurosci. 9:410–413.

Galletti C, Fattori P, Kutz DF, Gamberini M. 1999. Brain location and visual topography of cortical area V6A in the macaque monkey. Eur J Neurosci. 11:575–582.

Galletti C, Kutz DF, Gamberini M, Breveglieri R, Fattori P. 2003. Role of the medial parieto-occipital cortex in the control of reaching and grasping movements. Exp Brain Res. 153:158–170.

Gamberini M, Galletti C, Bosco A, Breveglieri R, Fattori P. 2011. Is the medial posterior parietal area V6A a single functional area? J Neurosci. 31:5145–5157.

Gamberini M, Passarelli L, Fattori P, Zucchelli M, Bakola S, Luppino G, Galletti C. 2009. Cortical connections of the visuomotor parietooccipital area V6Ad of the macaque monkey. J Comp Neurol. 513:622–642.

Genovesio A, Brasted PJ, Mitz AR, Wise SP. 2005. Prefrontal cortex activity related to abstract response strategies. Neuron. 47:307–320.

Genovesio A, Brasted PJ, Wise SP. 2006. Representation of future and previous spatial goals by separate neural populations in prefrontal cortex. J Neurosci. 26:7305–7316.

Gerbella M, Belmalih A, Borra E, Rozzi S, Luppino G. 2007. Multimodal architectonic subdivision of the caudal ventrolateral prefrontal cortex of the macaque monkey. Brain Struct Funct. 212:269–301.

Gerbella M, Belmalih A, Borra E, Rozzi S, Luppino G. 2010. Cortical connections of the macaque caudal ventrolateral prefrontal areas 45A and 45B. Cereb Cortex. 20:141–168.

Gerbella M, Belmalih A, Borra E, Rozzi S, Luppino G. 2011. Cortical connections of the anterior (F5a) subdivision of the macaque ventral premotor area F5. Brain Struct Funct. 216:43–65.

Gerbella M, Borra E, Mangiaracina C, Rozzi S, Luppino G. 2016. Corticostriate projections from areas of the “lateral grasping network”: evidence for multiple hand-related input channels. Cereb Cortex. 26:3096–3115.

Gerbella M, Borra E, Tonelli S, Rozzi S, Luppino G. 2013. Connectional heterogeneity of the ventral part of the macaque area 46. Cereb Cortex. 23:967–987.

Ghazanfar A, Nielsen K, Logothetis NK. 2006. Eye movements of monkey observers viewing vocalizing conspecifics. Cognition. 101:515–529.

Goldman-Rakic PS. 1987. Motor control function of the prefrontal cortex. Ciba Found Symp. 132:187–200.

Gregoriou GG, Borra E, Matelli M, Luppino G. 2006. Architectonic organization of the inferior

parietal convexity of the macaque monkey. J Comp Neurol. 496:422–451.

Hadjidimitrakis K, Bertozzi F, Breveglieri R, Bosco A, Galletti C, Fattori P. 2014. Common neural substrate for processing depth and direction signals for reaching in the monkey medial posterior parietal cortex. Cereb Cortex. 24:1645–1657.

Hasegawa RP, Blitz AM, Goldberg ME. 2004. Neurons in monkey prefrontal cortex whose activity tracks the progress of a three-step self-ordered task. J Neurophysiol. 92:1524–1535.

Hoshi E, Tanji J. 2004. Area-selective neuronal activity in the dorsolateral prefrontal cortex for information retrieval and action planning. J Neurophysiol. 91:2707–2722.

Huerta MF, Krubitzer LA, Kaas JH. 1987. Frontal eye field as defined by intracortical microstimulation in squirrel monkeys, owl monkeys, and macaque monkeys II. cortical connections. J Comp Neurol. 265:332–361.

Ibos G, Duhamel JR, Ben Hamed S. 2013. A functional hierarchy within the parietofrontal network in stimulus selection and attention control. J Neurosci. 33:8359-69.

Ichihara-Takeda S, Funahashi S. 2007. Activity of primate orbitofrontal and dorsolateral prefrontal neurons: task-related activity during an oculomotor delayed-response task. Exp brain Res. 181:409–425.

Jellema T, Baker CII, Wicker B, Perrett DII. 2000. Neural representation for the perception of the intentionality of actions. Brain Cogn. 44:280–302.

Kaas JH, Hackett TA. 2000. Subdivisions of auditory cortex and processing streams in primates. Proc Natl Acad Sci U S A. 97:11793–11799.

Koechlin E, Summerfield C. 2007. An information theoretical approach to prefrontal executive function. Trends Cogn Sci. 11:229–235.

Kravitz DJ, Saleem KS, Baker CI, Mishkin M. 2011. A new neural framework for visuospatial processing. Nat Rev Neurosci. 12:217–230.

Krueger F, Moll J, Zahn R, Heinecke A, Grafman J. 2007. Event frequency modulates the processing of daily life activities in human medial prefrontal cortex. Cereb Cortex 17:2346-

2353;

Kutz DF, Fattori P, Gamberini M, Breveglieri R, Galletti C. 2003. Early- and late-responding cells to saccadic eye movements in the cortical area V6A of macaque monkey. Exp brain Res. 149:83–95.

Leichnetz GR. 2001. Connections of the medial posterior parietal cortex (area 7m) in the monkey. Anat Rec. 263:215–236.

Levy R, Goldman-Rakic PS. 2000. Segregation of working memory functions within the dorsolateral prefrontal cortex. Exp Brain Res. 133:23–32.

Luppino G, Ben Hamed S, Gamberini M, Matelli M, Galletti C. 2005. Occipital (V6) and parietal (V6A) areas in the anterior wall of the parieto-occipital sulcus of the macaque: A cytoarchitectonic study. Eur J Neurosci. 21:3056–3076.

Luppino G, Calzavara R, Rozzi S, Matelli M. 2001. Projections from the superior temporal sulcus to the agranular frontal cortex in the macaque. Eur J Neurosci. 14:1035–1040.

Luppino G, Gerbella M, Rozzi S, Borra E. 2014. Involvement of the macaque prefrontal area 46d in a cortical network for controlling visually guided reaching-grasping movements. Federation of European Neuroscience Societies (FENS) Forum, 2014. Milan, Italy.

Luppino G, Matelli M, Camarda R, Rizzolatti G. 1993. Corticocortical connections of area F3 (SMA-proper) and area F6 (pre-SMA) in the macaque monkey. J Comp Neurol. 338:114–140.

Luppino G, Rozzi S, Calzavara R, Matelli M. 2003. Prefrontal and agranular cingulate projections to the dorsal premotor areas F2 and F7 in the macaque monkey. Eur J Neurosci. 17:559–578.

Lynch JC, Tian J-R. 2006. Cortico-cortical networks and cortico-subcortical loops for the higher control of eye movements. Prog Brain Res. 151:461–501.

Marconi B, Genovesio A, Battaglia-Mayer A, Ferraina S, Squatrito S, Molinari M, Lacquaniti F, Caminiti R. 2001. Eye-hand coordination during reaching. I. Anatomical relationships between parietal and frontal cortex. Cereb Cortex. 11:513–527.

Matelli M, Govoni P, Galletti C, Kutz DF, Luppino G. 1998. Superior area 6 afferents from the

superior parietal lobule in the macaque monkey. J Comp Neurol. 402:327–352.

Mistlin AJ, Perrett DI. 1990. Visual and somatosensory processing in the macaque temporal cortex: the role of “expectation”. Exp brain Res. 82:437–450.

Morecraft RJ, Cipolloni PB, Stilwell-Morecraft KS, Gedney MT, Pandya DN. 2004. Cytoarchitecture and cortical connections of the posterior cingulate and adjacent somatosensory fields in the rhesus monkey. J Comp Neurol. 469:37–69.

Nachev P, Kennard C, Husain M. 2008. Functional role of the supplementary and pre-supplementary motor areas. Nat Rev Neurosci. 9:856–869.

Ninokura Y, Mushiake H, Tanji J. 2004. Integration of temporal order and object information in the monkey lateral prefrontal cortex. J Neurophysiol. 91.

Olson CR, Musil SY, Goldberg ME. 1996. Single neurons in posterior cingulate cortex of behaving macaque: eye movement signals. J Neurophysiol. 76:3285–3300.

Pandya DN, Seltzer B. 1982. Intrinsic connections and architectonics of posterior parietal cortex in the rhesus monkey. J Comp Neurol. 204:196–210.

Passarelli L, Rosa MGP, Bakola S, Gamberini M, Worthy KH, Fattori P, Galletti C. 2017. Uniformity and diversity of cortical projections to precuneate areas in the macaque monkey : what de fi nes area PGm ? Cereb Cortex. Mar 25:1-18. doi: 10.1093/cercor/bhx067.

Passarelli L, Rosa MGP, Gamberini M, Bakola S, Burman KJ, Fattori P, Galletti C. 2011. Cortical connections of area V6Av in the macaque: a visual-input node to the eye/hand coordination system. J Neurosci. 31:1790–1801.

Petrides M, Pandya DN. 1988. Association fiber pathways to the frontal cortex from the superior temporal region in the rhesus monkey. J Comp Neurol. 273:52–66.

Petrides M, Pandya DN. 1999. Dorsolateral prefrontal cortex : comparative cytoarchitectonic analysis in the human and the macaque brain and corticocortical connection patterns. 11:1011–1036.

Picard N, Strick PL. 2001. Imaging the premotor areas. Curr Opin Neurobiol. 11:663–672.

Rao SC, Rainer G, Miller EK. 1997. Integration of what and where in the primate prefrontal cortex. Science. 276:821–824.

Raos V, Umiltá M-A, Gallese V, Fogassi L. 2004. Functional properties of grasping-related neurons in the dorsal premotor area F2 of the macaque monkey. J Neurophysiol. 92:1990–2002.

Requin J, Lecas J-C, Vitton N. 1990. A comparison of preparation-related neuronal activity changes in the prefrontal, premotor, primary motor and posterior parietal areas of the monkey cortex: preliminary results. Neurosci Lett. 111:151–156.

Romanski LM, Averbeck BB. 2009. The primate cortical auditory system and neural representation of conspecific vocalizations. Annu Rev Neurosci. 32:315–346.

Rozzi S, Calzavara R, Belmalih A, Borra E, Gregoriou GG, Matelli M, Luppino G. 2006. Cortical connections of the inferior parietal cortical convexity of the macaque monkey. Cereb Cortex. 16:1389–1417.

Saleem KS, Logothetis NK. 2012. A combined MRI and histology atlas of the rhesus monkey brain in stereotaxic coordinates. 2nd edition with horizontal, coronal, and sagittal series. San Diego: Academic Press/Elsevier.

Saleem KS, Kondo H, Price JL. 2008. Complementary circuits connecting the orbital and medial prefrontal networks with the temporal, insular, and opercular cortex in the macaque monkey. J Comp Neurol. 506:659–693.

Saleem KS, Miller B, Price JL. 2014. Subdivisions and connectional networks of the lateral prefrontal cortex in the macaque monkey. J Comp Neurol. 522:1641–1690.

Sato N, Sakata H, Tanaka YL, Taira M. 2010. Context-dependent place-selective responses of the neurons in the medial parietal region of macaque monkeys. Cereb Cortex. 20:846–858.

Schall JD, Morel A, King DJ, Bullier J. 1995. Topography of visual cortex connections with frontal eye field in macaque: convergence and segregation of processing streams. J Neurosci. 15:4464–4487.

Seltzer B, Pandya DN. 1989. Frontal lobe connections of the superior temporal sulcus in the rhesus

monkey. J Comp Neurol. 281:97–113.

Sigala N, Kusunoki M, Nimmo-Smith I, Gaffan D, Duncan J. 2008. Hierarchical coding for sequential task events in the monkey prefrontal cortex. Proc Natl Acad Sci U S A. 105:11969–11974.

Stanton GB, Bruce CJ, Goldberg ME. 1993. Topography of projections to the frontal lobe from the macaque frontal eye fields. J Comp Neurol. 330:286–301.

Stanton GB, Bruce CJ, Goldberg ME. 1995. Topography of projections to posterior cortical areas from the macaque frontal eye fields. J Comp Neurol. 353:291–305.

Sugihara T, Diltz MD, Averbeck BB, Romanski LM. 2006. Integration of auditory and visual communication information in the primate ventrolateral prefrontal cortex. J Neurosci. 26:11138–11147.

Takahara D, Inoue K-I, Hirata Y, Miyachi S, Nambu A, Takada M, Hoshi E. 2012. Multisynaptic projections from the ventrolateral prefrontal cortex to the dorsal premotor cortex in macaques - anatomical substrate for conditional visuomotor behavior. Eur J Neurosci. 36:3365–3375.

Tanji J, Hoshi E. 2008. Role of the lateral prefrontal cortex in executive behavioral control. Physiol Rev. 88:37–57.

Tate AJ, Fischer H, Leigh AE, Kendrick KM. 2006. Behavioural and neurophysiological evidence for face identity and face emotion processing in animals. Philos Trans R Soc B Biol Sci. 361:2155–2172.

Thompson KG, Bichot NP. 2005. A visual salience map in the primate frontal eye field. Prog Brain Res. 147:251-62.

Tsujimoto S, Genovesio A, Wise SP. 2011. Comparison of strategy signals in the dorsolateral and orbital prefrontal cortex. J Neurosci. 31:4583–4592.

Vaadia E, Benson DA, Hienz RD, Goldstein MH. 1986. Unit study of monkey frontal cortex: active localization of auditory and of visual stimuli. J Neurophysiol. 56:934–952.

Walker E. 1940. A cytoarchitectural study of the prefrontal area of the macaque monkey. J Comp

Neurol. 73:59–86.

Wendelken C, Nakhabenko D, Donohue SE, Carter CS, Bunge SA. 2008. "Brain is to thought as stomach is to ??": Investigating the role of rostrolateral prefrontal cortex in relational reasoning. J. Cogn Neurosci. 20:682-693

Yamagata T, Nakayama Y, Tanji J, Hoshi E. 2012. Distinct information representation and processing for goal-directed behavior in the dorsolateral and ventrolateral prefrontal cortex and the dorsal premotor cortex. J Neurosci. 32:12934–12949.

Table 1: Animals used, location of injection sites and type and amount of injected tracers.

Case	**Species**	**Sex**	**Age (years)**	**Weight (kg)**	**Hemisph.**	**Area**	mm*	**Tracer**	**Amount**
23	*M. fascicularis*	M	7	6	L	46d	2.5	DY 2%	2 x 0,3 µl
57	*M. fascicularis*	M	5	3,4	R	46d	3.5	WGA 4%	0,3 µl
58	*M. fascicularis*	F	6	3	R	8r	-	DY 2%	0,25 µl
					R	46d	1.5	FB 3%	0,2 µl
60	*M. fascicularis*	M	4	3,2	L	8r	-	CTB-green 1%	1,8 µl
					L	46d	3	FB 3%	0,3 µl
					L	46d	5.5	CTB-red 1%	2 µl
					R	46d	2.5	FR 10%	1,8 µl
					R	46d	4.5	LYD 10%	2 µl
64	*M fascicularis*	F	4	3,1	R	46d	8	DY 2%	0,2 µl
					L	46d	5.5	FR 10%	2 x 0,8 µl
					L	46d	8	LYD 10%	2 x 0,8 µl
					L	46d	11	CTB-green 1%	2 x 0,75 µl

*mm from areas 8r/46d border

Table 2: Percent distribution (%) and total number (n) of labeled neurons observed following representative injections in area 8r and in caudal, middle and rostral area 46d.

	Area 8r		Caudal 46d		Middle 46d			Rostral 46d	
Case	60l CTBg	58r DY	58r FB	23l DY	57r WGA	60l FB	60l CTBr	64r DY	64l CTBg
	%	%	%	%	%	%	%	%	%
Prefrontal									
10	-	-	*	-	-	-	1.9	7.6	19.9
9	-	-	1.6	3.5	1.3	3.2	13.7	25.8	15.1
8B	1.5	*	15.3	8.3	3.0	7.7	21.7	5.0	2.7
46d	20.2	7.5	/	/	/	/	/	/	/
46vr	-	1.4	2.6	-	1	1.9	7.9	5.2	3.0
46vc	-	5.0	1.3	*	10.4	10.1	4.5	-	-
46f	2.0	2.5	5.4	16.3	9.6	11.9	1.9	8.3	8.4
8r	/	/	5.0	11.4	1.1	4.4	1.2	11.3	8.2
8A	7.9	3.4	8.1	10.4	*	4.2	1.9	2.7	2.2
8-FEF	38.1	50.7	20.3	17.6	*	2.9	-	11.9	9.6
45B	1.0	1.7	1.4	-	-	2.1	1.2	1.0	-
45A; 12l; 12r	10.4	5.2	*	-	-	1.1	2.3	3.1	9.8
Orbitofrontal	-	-	-	-	*	*	*	-	1.8
total prefrontal	*81.4*	*78.2*	*62.2*	*68.5*	*28.2*	*50.1*	*59.3*	*82.0*	*80.9*
Caudal Frontal									
F7-SEF; F7-non SEF	3.4	1.9	3.4	10.7	17.0	18.2	19.5	-	2.8
F2	-	-	-	-	12.9	7.6	2.5	-	-
F6	-	-	-	-	6.0	8.3	6.2	-	-
F5	-	-	-	-	2.9	3.3	-	-	-
GrFO	-	-	-	2.1	2.2	1.3	-	-	-
total caudal frontal	*3.4*	*1.9*	*3.6*	*13.0*	*41.0*	*38.7*	*28.4*	-	*2.8*
Temporal									
STP	1.2	5.1	4.0	-	-	-	-	7.5	8.5
STG	-	-	-	-	-	-	-	2.3	3.0
FST	*	1.7	-	-	-	-	-	*	-
total temporal	*1.7*	*7.0*	*4.2*	-	-	-	-	*10.7*	*11.9*
Parietal									
LIP	9.3	10.8	4.3	4.2	*	-	-	-	-
PG; Opt	-	-	2.7	-	6.1	2.1	-	*	*
PGm	-	-	3.0	3.7	1.0	1.9	4.9	-	-
V6A	-	-	11.6	3.3	6.1	3.9	*	-	-
MST	2.1	1.4	*	-	2.0	-	-	-	-
total parietal	*11.8*	*12.4*	*22.1*	*11.4*	*15,7*	*8.2*	*5.8*	1.1	*
Cingulate									
Rostral (24)	-	-	*	2.5	7.3	1.4	1.3	-	-
Caudal (23, 31)	-	-	6.6	4.5	4.9	1.1	4.7	6.0	2.8
Other	1.4	-	*	-	2.4	-	-	-	*
total cell n.	4715	1842	18667	8745	27468	24905	24993	8514	20238

Note: *= labeling <1%; - = no labeling (or <0.5%).

Figure legends

Figure 1. Injections in areas 46d and 8r. (A) Composite view of all the injection sites mapped on a template hemisphere (Case 23l). Each injection site in area 46d was reported on the template hemisphere based on its distance from the caudal border of this area; the two injection sites in area 8r were reported based on their location within this area with respect to the caudal end of the principal sulcus. Injection sites placed in area 46d are shown as white, gray or black circles according to their location in the caudal, middle, and rostral area 46d sector, respectively; injection sites placed in area 8r are shown as white squares. Dashed lines mark cytoarchitectonic borders. (B) FB injection in the caudal area 46d sector in Case 58r; (C) FB injections in the middle area 46d sector in Case 60l; (D) CTBr injection in the middle area 46d sector in Case 60l; (E) CTBg injection in the rostral area 46d sector in Case 64l. Arrowheads mark the border of area 46d with areas 8B, or 9. Dashed line in B-E marks the grey/white matter border. Scale bar in B applies to B-E. IA: inferior arcuate sulcus; SA: superior arcuate sulcus; P: principal sulcus.

Figure 2. Cytoarchitecture of area 46d and adjacent areas. A-C: Low-power photomicrographs of a series of Nissl-stained coronal sections, in a caudal to rostral order, taken from Case 36r. Arrows indicate the borders between cytoarchitectonic areas. The levels at which the sections were taken are indicated by dashed lines on the drawing of the dorsolateral view of the hemisphere in D. Boxes in the section drawings indicate the locations of the photomicrographs in A-C. Dashed boxes in A, B, and C indicate the location of the higher magnification views in E-H. Scale bar in A applies also to B and C. Scale bar in E applies also to F-H. Abbreviations as in Figure 1.

Figure 3. Distribution of the retrograde labeling observed after injections in the caudal area 46d sector in Cases 58r FB and 23l DY. The labeling is shown in dorsolateral and medial views of the 3D reconstructions of the injected hemispheres (A) and in drawings of coronal sections from Case 58r FB (B). Sections are shown in a rostral to caudal order (a–n). The dorsolateral view of the injected hemisphere in the top left part of B shows the levels at which the sections were taken and

the location of the injection site. Each dot corresponds to one labeled neuron. C: Central sulcus; Ca: calcarine fissure; Cg: cingulate sulcus; IO: inferior occipital sulcus; IP: intraparietal sulcus; L: lateral fissure; LO: lateral orbital sulcus; Lu: lunate sulcus; MO: medial orbital sulcus; OT: occipito-temporal sulcus; ST: superior temporal sulcus. Other abbreviations as in Figure 1.

Figure 4. Distribution of the retrograde labeling observed following injections in the middle area 46d sector more caudally (Cases 60l FB and 57r WGA) and more rostrally (Case 60l CTBr). The labeling is shown in dorsolateral, medial, and ventral views of the 3D reconstructions of the injected hemispheres. Other conventions and abbreviations as in Figures 1 and 3.

Figure 5. Distribution of the retrograde labeling observed in Case 60l FB (A) and in Case 60l CTBr (A') shown in drawings of coronal sections. Conventions and abbreviations as in Figures 1 and 3.

Figure 6. Distribution of the retrograde labeling observed in Cases 64r DY and 64l CTBg following injections in the rostral area 46d sector. The labeling is shown in dorsolateral, medial, and ventral views of the 3D reconstructions of the injected hemispheres (A) and in 2D reconstructions of the STS (B). Each 2D reconstruction of the STS was aligned to correspond with the fundus and middle of the floor (dotted lines). The continuous lines indicate the lips of the sulcus and the upper and lower edges of the floor. Conventions and abbreviations as in Figures 1 and 3.

Figure 7. Distribution of the retrograde labeling observed in Case 64l CTBg, shown in drawings of coronal sections. Conventions and abbreviations as in Figures 1 and 3.

Figure 8. Examples of laminar patterns of retrograde and anterograde labeling observed following injections in area 46d. In each photomicrograph is indicated the area in which the labeling was observed and, in parentheses, the injected sector of area 46d. A is taken from Case 64l LYD; B from Case 58r FB; C and F from Case 60l FB; D from Case 60 LYD; E and J from Case 64l CTBg; G from Case 60l CTBr; H and I from Case 60r FR. Scale bar in A applies also to B-E and G-J.

Figure 9. Distribution of the labeling observed in Case 60l CTBg following injection in dorsal area 8r, shown in a dorsolateral view of the 3D reconstructions of the injected hemisphere (A), in

drawings of coronal sections (B) and in 2D reconstructions of the STS (C). PMT: posterior middle temporal sulcus. Conventions and other abbreviations as in Figures 1 and 3.

Figure 10. Mean percent distribution of the retrograde labeling observed in the cases of injections in the different sectors of area 46d shown in Table 2. The data are shown in terms of areal distribution in A-C and of regional distribution in D. In D, the frontal motor region includes the caudal frontal areas and the oculomotor area 8-FEF.

Figure 11. Summary view of the cortical connectivity of the connectionally distinct area 46d sectors identified in the present study. A-C: drawings of an hemisphere showing the major sources of ipsilateral cortical projections to each sector. The injected sectors are indicated by a black zone. Based on qualitative and quantitative analysis of the distribution of the retrograde labeling, more strongly and less strongly connected areas are shown in darker and lighter gray, respectively. D: general organization of the lateral prefrontal cortex, as it emerges from the present and previous studies (Gerbella et al., 2010; 2013; Borra et al., 2011).

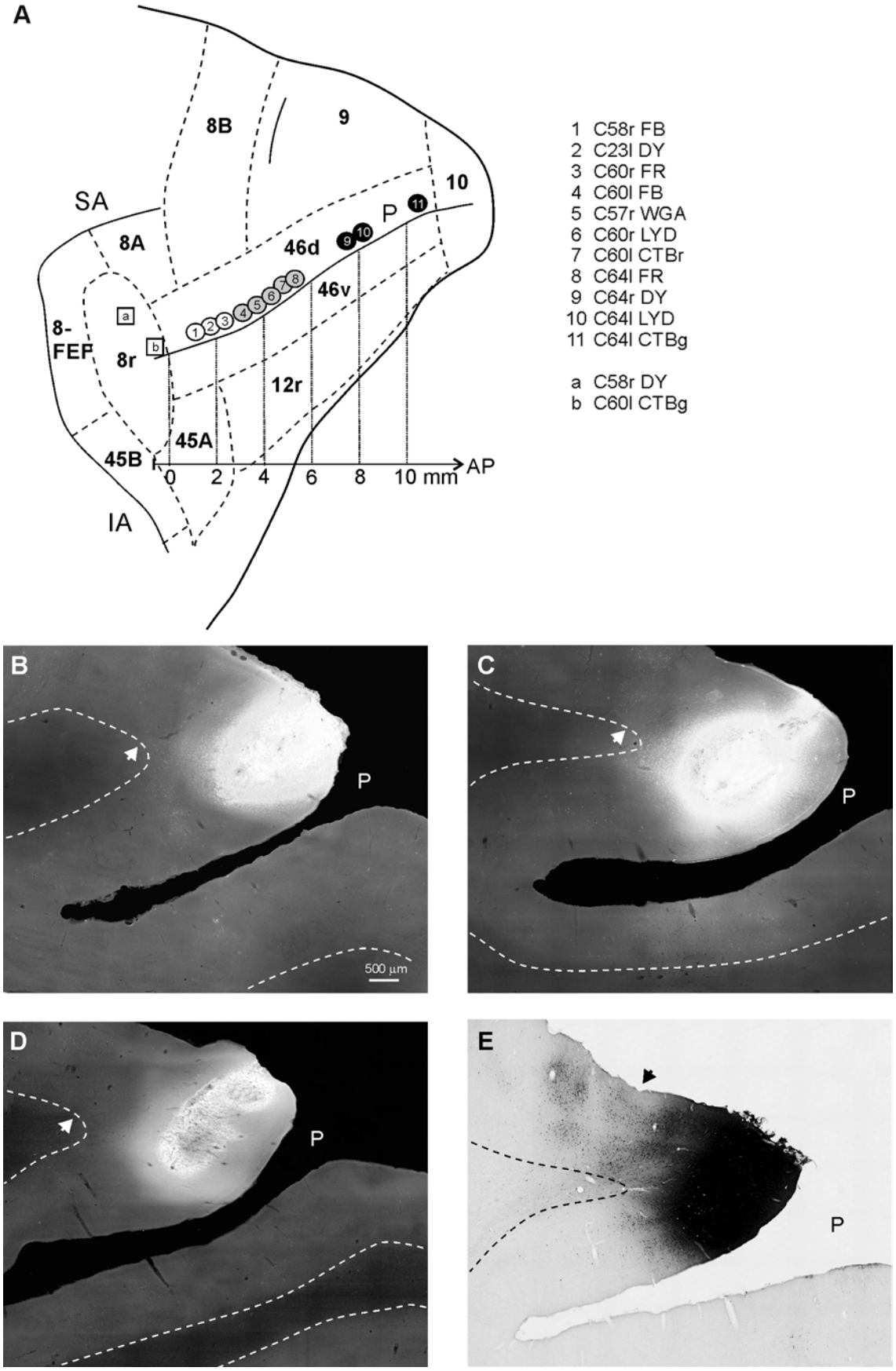
A
8B
9
10
SA
P
8A
46d
46v
8-
FEF
8r
12r
45A
45B
IA
0
2
4
6
8
10 mm
AP
1 C58r FB
2 C23l DY
3 C60r FR
4 C60l FB
5 C57r WGA
6 C60r LYD
7 C60l CTBr
8 C64l FR
9 C64r DY
10 C64l LYD
11 C64l CTBg
a C58r DY
b C60l CTBg
B
C
D
E
P
500 µm

Figure1

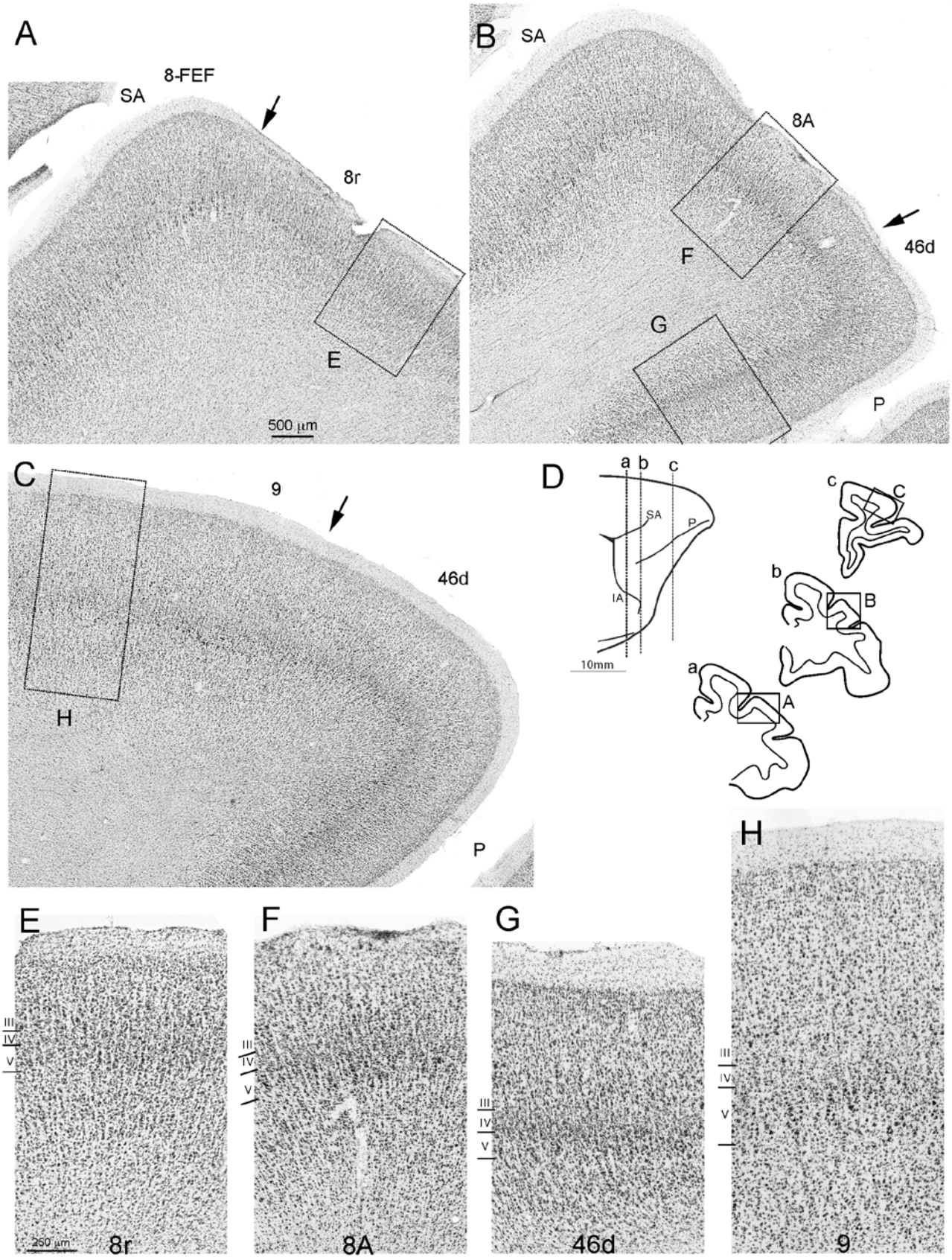
A
8-FEF
SA
8r
E
500 µm
B
SA
8A
F
46d
G
P
C
9
46d
H
P
D
a
b
c
SA
P
IA
10mm
c
C
b
B
a
A
E
III
IV
V
250 µm
8r
F
III
IV
V
8A
G
III
IV
V
46d
H
III
IV
V
9

Figure 2

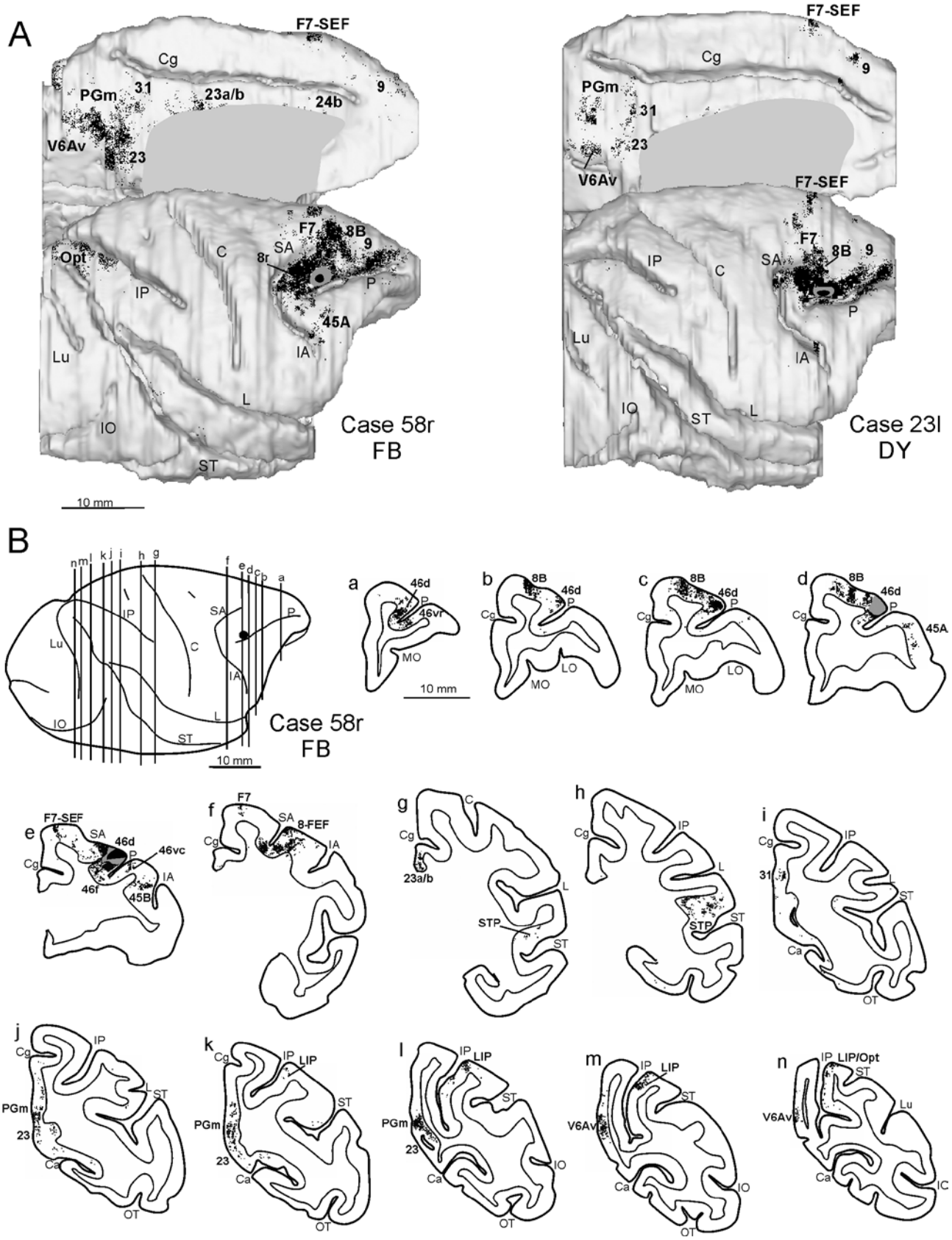
A
F7-SEF
Cg
PGm
31
23a/b
24b
9
V6Av
23
F7
8B
9
Opt
C
SA
8r
P
IP
45A
Lu
IA
L
IO
ST
Case 58r
FB
10 mm
F7-SEF
Cg
9
PGm
31
23
V6Av
F7-SEF
F7
8B
9
IP
C
SA
P
Lu
IA
IO
ST
L
Case 23l
DY
B
nm l k j i h g f e d c b a
IP
SA
P
Lu
C
IA
IO
L
ST
Case 58r
FB
10 mm
a
46d
P
46vr
MO
10 mm
b
8B
46d
P
Cg
LO
MO
c
8B
46d
P
Cg
LO
MO
d
8B
46d
P
Cg
45A
e
F7-SEF
SA
46d
P
46vc
Cg
IA
46f
45B
f
F7
SA
8-FEF
Cg
IA
g
C
Cg
23a/b
L
STP
ST
h
IP
Cg
L
STP
ST
i
IP
Cg
31
ST
Ca
OT
j
IP
Cg
L
ST
PGm
23
Ca
OT
k
IP
LIP
Cg
ST
PGm
23
Ca
OT
l
IP
LIP
ST
PGm
23
Ca
IO
OT
m
IP
LIP
ST
V6Av
Ca
IO
OT
n
IP
LIP/Opt
ST
Lu
V6Av
Ca
IC

Figure 3

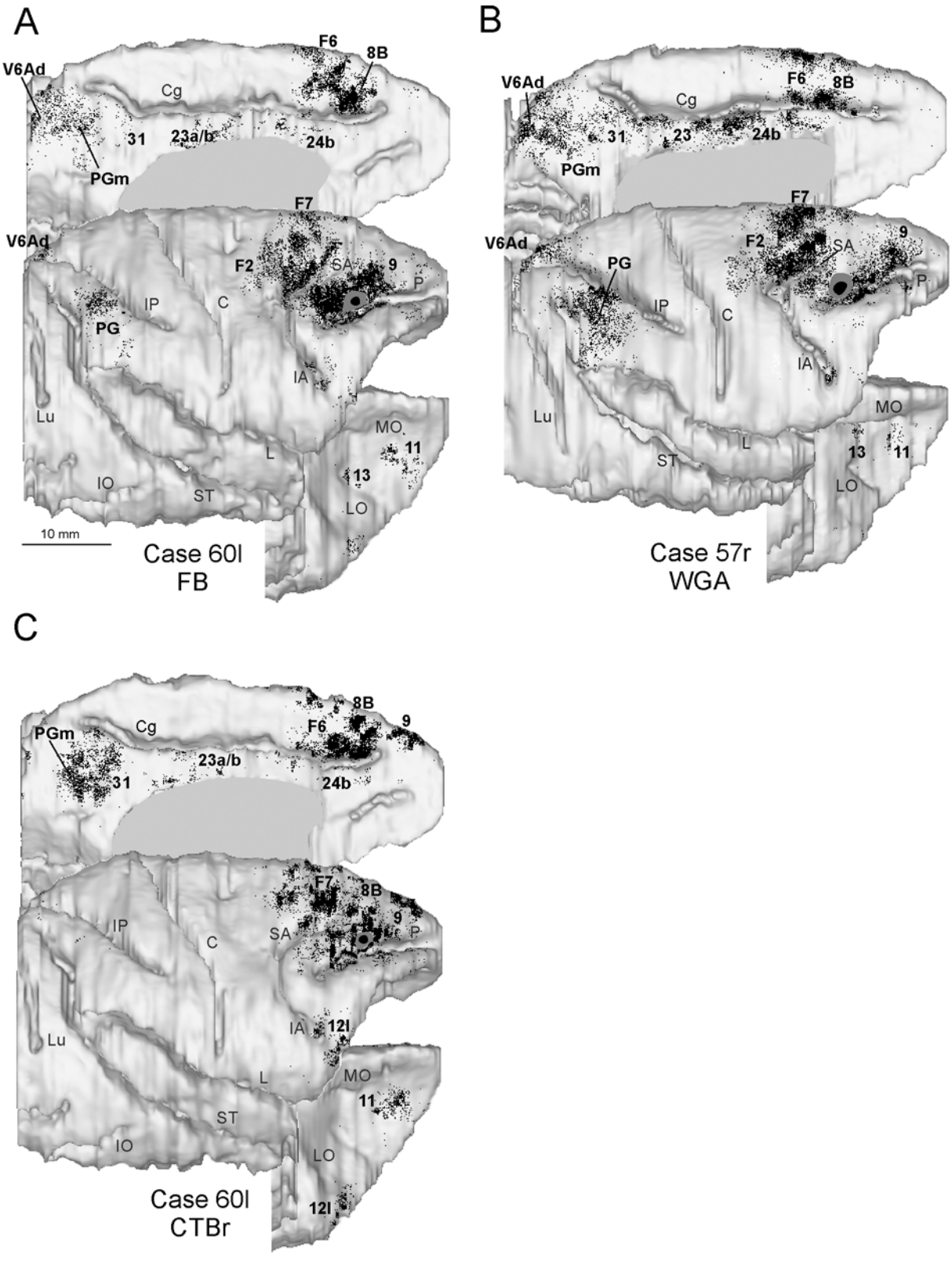
A
V6Ad
F6
8B
Cg
31
23a/b
24b
PGm
F7
V6Ad
F2
SA
9
P
IP
C
PG
IA
Lu
MO
11
L
13
IO
ST
LO
10 mm
Case 60l
FB
B
V6Ad
F6
8B
Cg
31
23
24b
PGm
F7
V6Ad
F2
SA
9
P
PG
IP
C
IA
Lu
MO
L
13
11
ST
LO
Case 57r
WGA
C
8B
PGm
Cg
F6
9
23a/b
31
24b
F7
8B
IP
C
SA
9
P
IA
12l
Lu
L
MO
11
ST
IO
LO
Case 60l
CTBr
12l

Figure 4

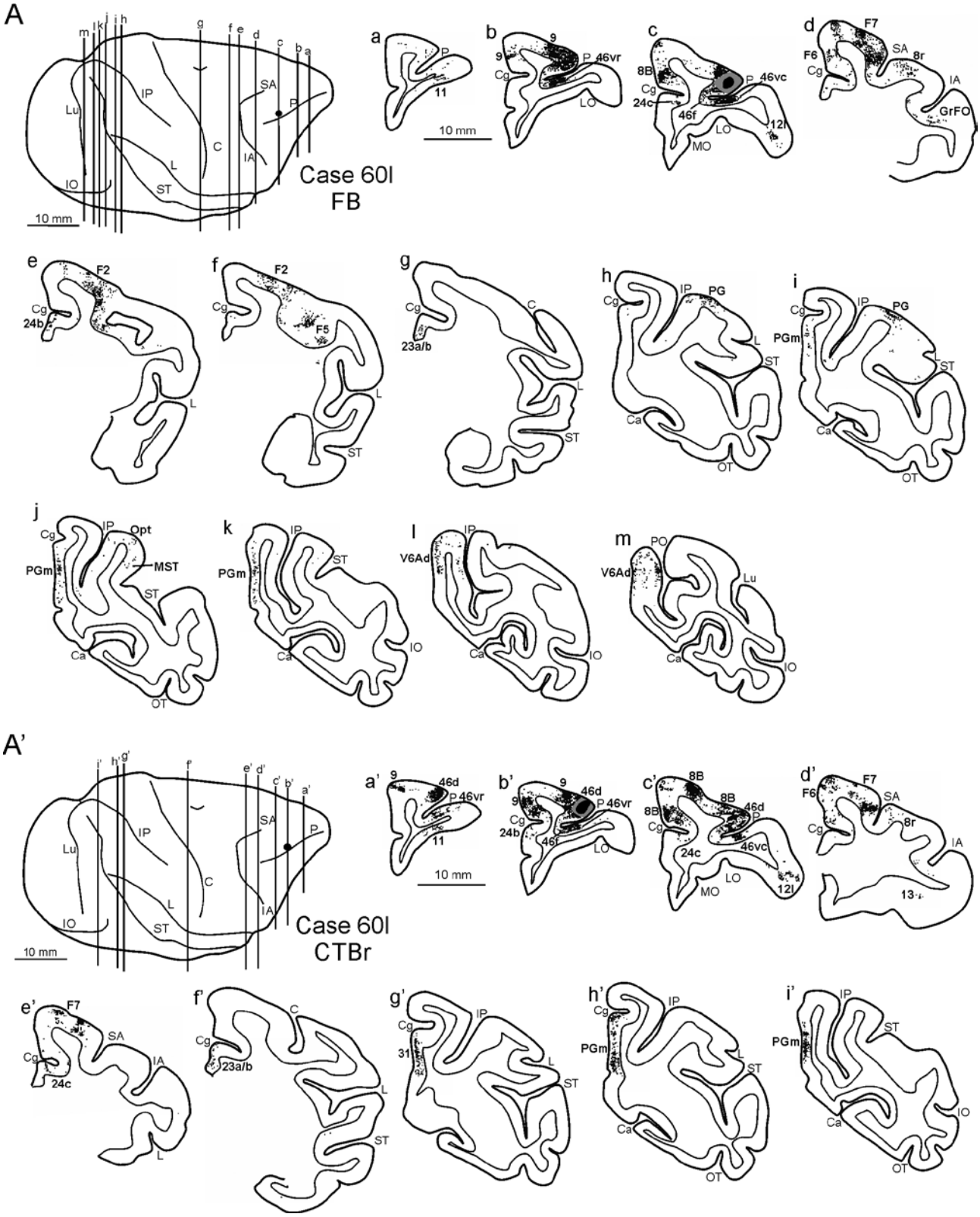
A
Case 60I
FB
10 mm
IP
Lu
IO
ST
SA
IA
L
C
P
a
b
c
d
9
11
46vr
46vc
LO
MO
8B
24c
46f
12l
F7
F6
8r
GrFO
e
f
g
h
i
F2
F5
24b
23a/b
PG
PGm
Ca
OT
j
k
l
m
Opt
MST
V6Ad
PO
A'
Case 60I
CTBr
a'
b'
c'
d'
46d
24b
13
e'
f'
g'
h'
i'
31

Figure 5

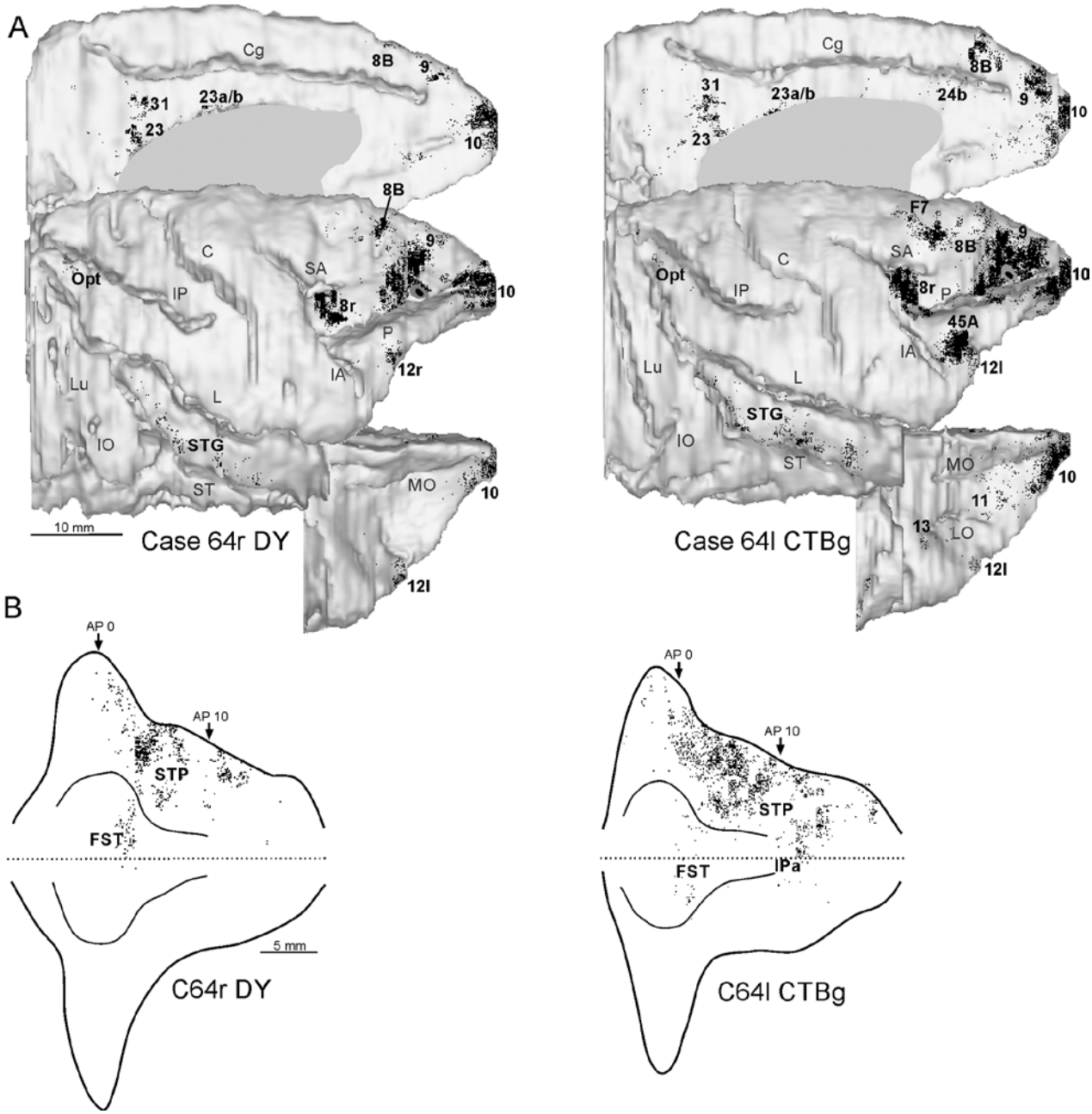
A
Cg
8B
9
31
23a/b
23
10
8B
C
SA
9
Opt
IP
8r
10
P
12r
IA
Lu
L
IO
STG
ST
MO
10
10 mm
Case 64r DY
12l
B
AP 0
AP 10
STP
FST
5 mm
C64r DY
Cg
8B
31
23a/b
24b
9
10
23
F7
9
C
SA
8B
Opt
IP
8r
P
10
45A
IA
12l
Lu
L
STG
IO
ST
MO
10
11
13
LO
12l
Case 64l CTBg
AP 0
AP 10
STP
FST
IPa
C64l CTBg

Figure 6

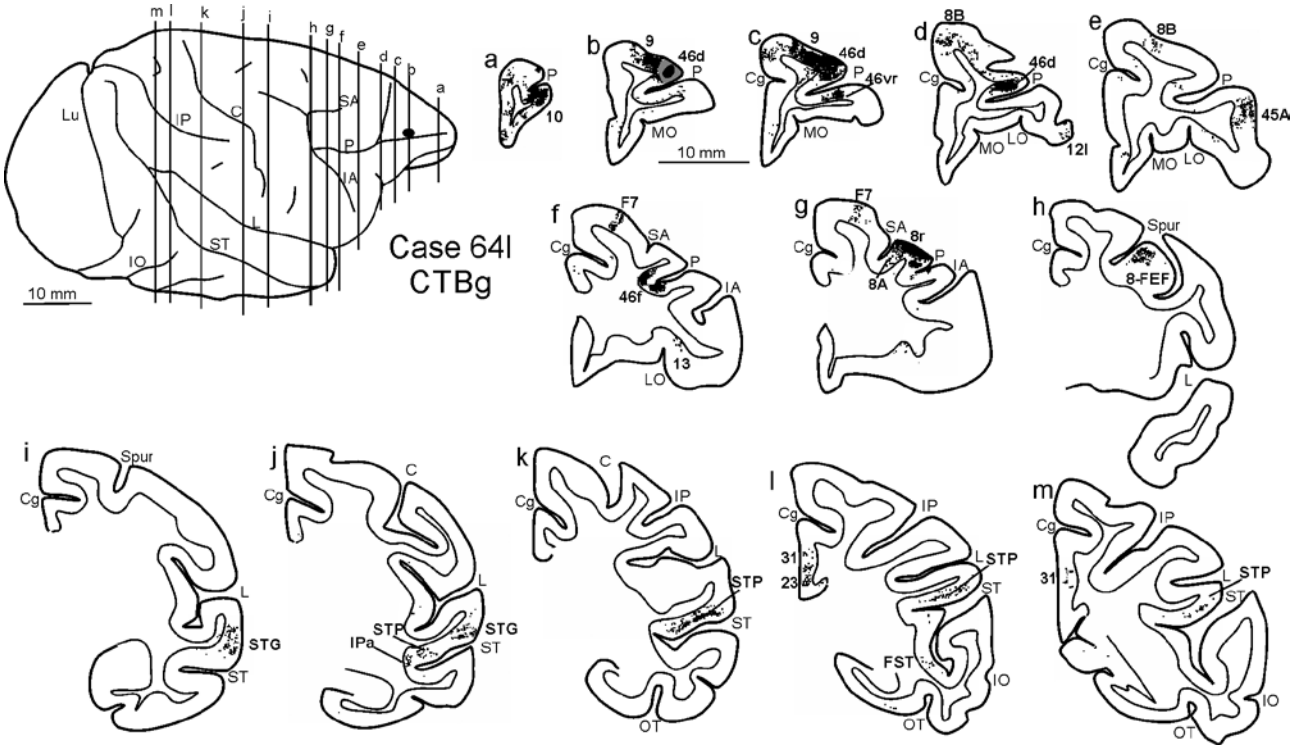
Case 64l
CTBg
10 mm
Lu
IP
C
SA
P
IA
L
ST
IO
m l k j i h g f e d c b a
a
P
10
b
9
46d
P
MO
10 mm
c
9
46d
P
46vr
MO
d
8B
46d
P
MO
LO
12l
e
8B
Cg
P
45A
MO
LO
f
F7
SA
Cg
P
46f
IA
13
LO
g
F7
SA
8r
Cg
P
IA
8A
h
Spur
Cg
8-FEF
L
i
Spur
Cg
L
STG
ST
j
C
Cg
L
STP
STG
IPa
ST
k
C
Cg
IP
L
STP
ST
OT
l
IP
Cg
31
23
LSTP
ST
FST
IO
OT
m
IP
Cg
31
L
STP
ST
IO
OT

Figure 7

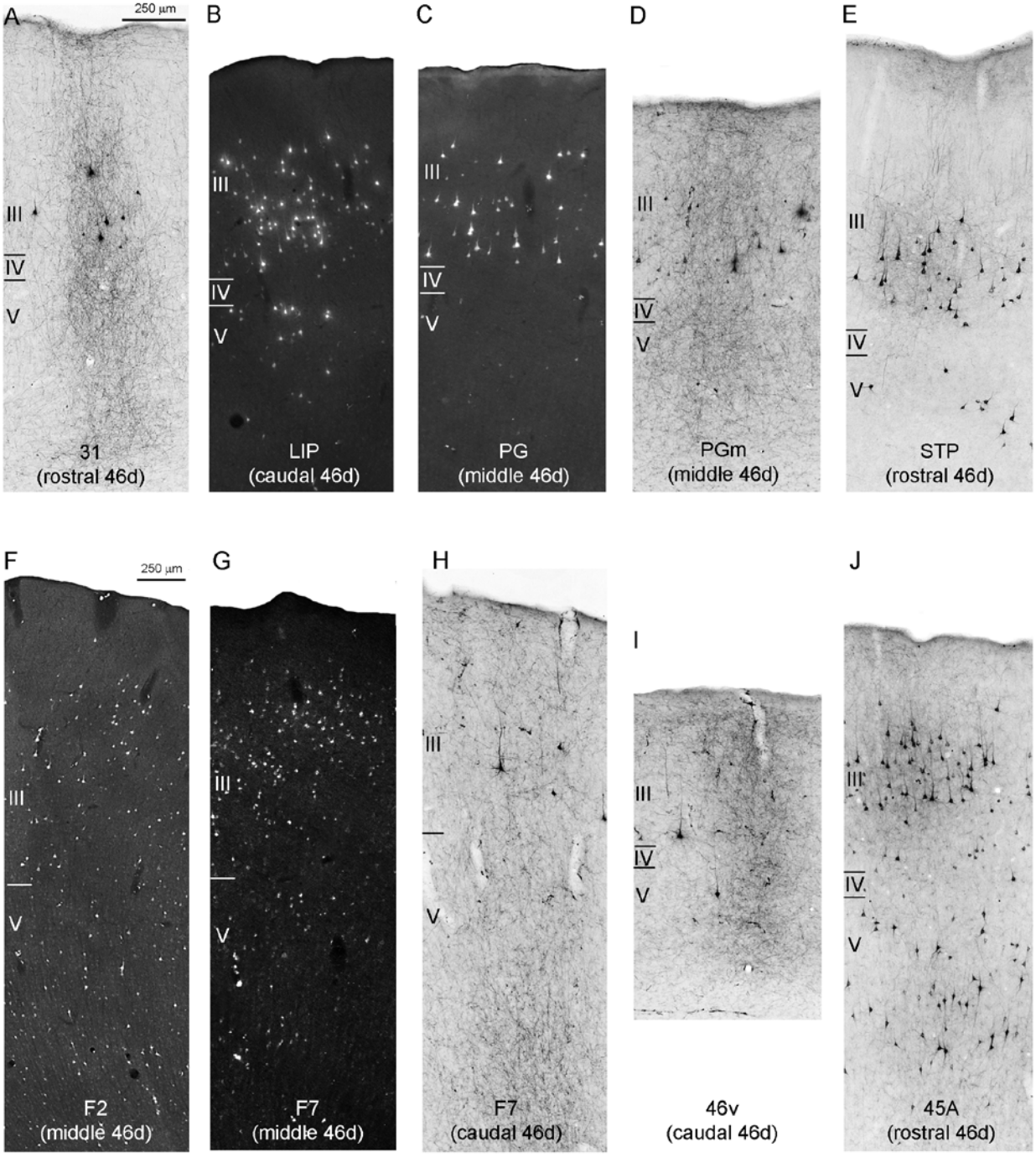
A
250 µm
III
IV
V
31
(rostral 46d)
B
III
IV
V
LIP
(caudal 46d)
C
III
IV
V
PG
(middle 46d)
D
III
IV
V
PGm
(middle 46d)
E
III
IV
V
STP
(rostral 46d)
F
250 µm
III
V
F2
(middle 46d)
G
III
V
F7
(middle 46d)
H
III
V
F7
(caudal 46d)
I
III
IV
V
46v
(caudal 46d)
J
III
IV
V
45A
(rostral 46d)

Figure 8

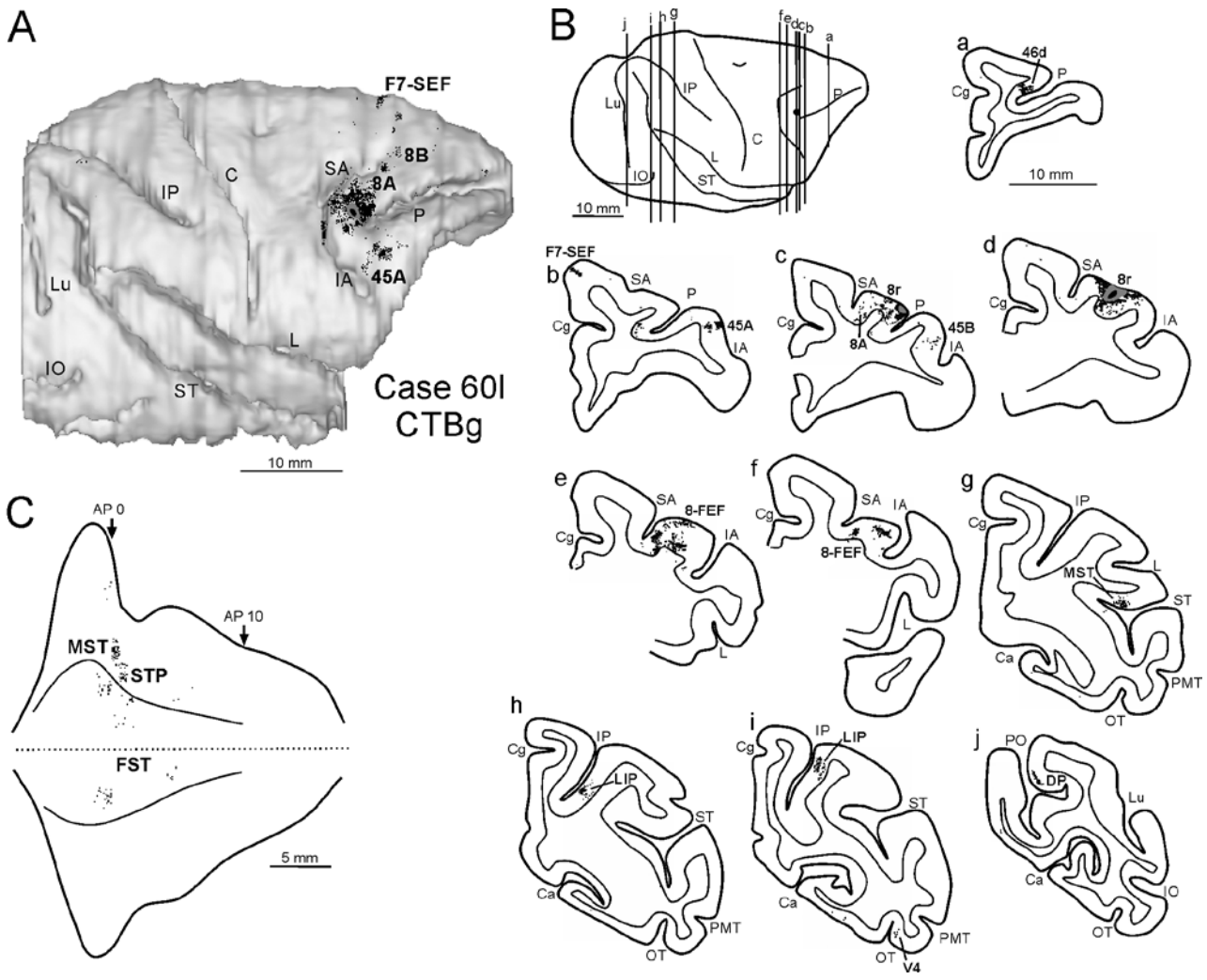
A
F7-SEF
8B
SA
8A
C
IP
P
IA
45A
Lu
L
IO
ST
Case 60l
CTBg
10 mm
B
j
i
h
g
f
e
d
c
b
a
Lu
IP
C
P
L
IO
ST
10 mm
a
46d
P
Cg
10 mm
F7-SEF
b
SA
P
Cg
45A
IA
c
SA
8r
P
Cg
8A
45B
IA
d
SA
8r
Cg
IA
e
SA
8-FEF
Cg
IA
L
f
SA
IA
Cg
8-FEF
L
g
IP
Cg
MST
L
ST
Ca
PMT
OT
h
Cg
IP
LIP
ST
Ca
PMT
OT
i
IP
LIP
Cg
ST
Ca
PMT
OT
V4
j
PO
LDP
Lu
Ca
IO
OT
C
AP 0
AP 10
MST
STP
FST
5 mm

Figure 9

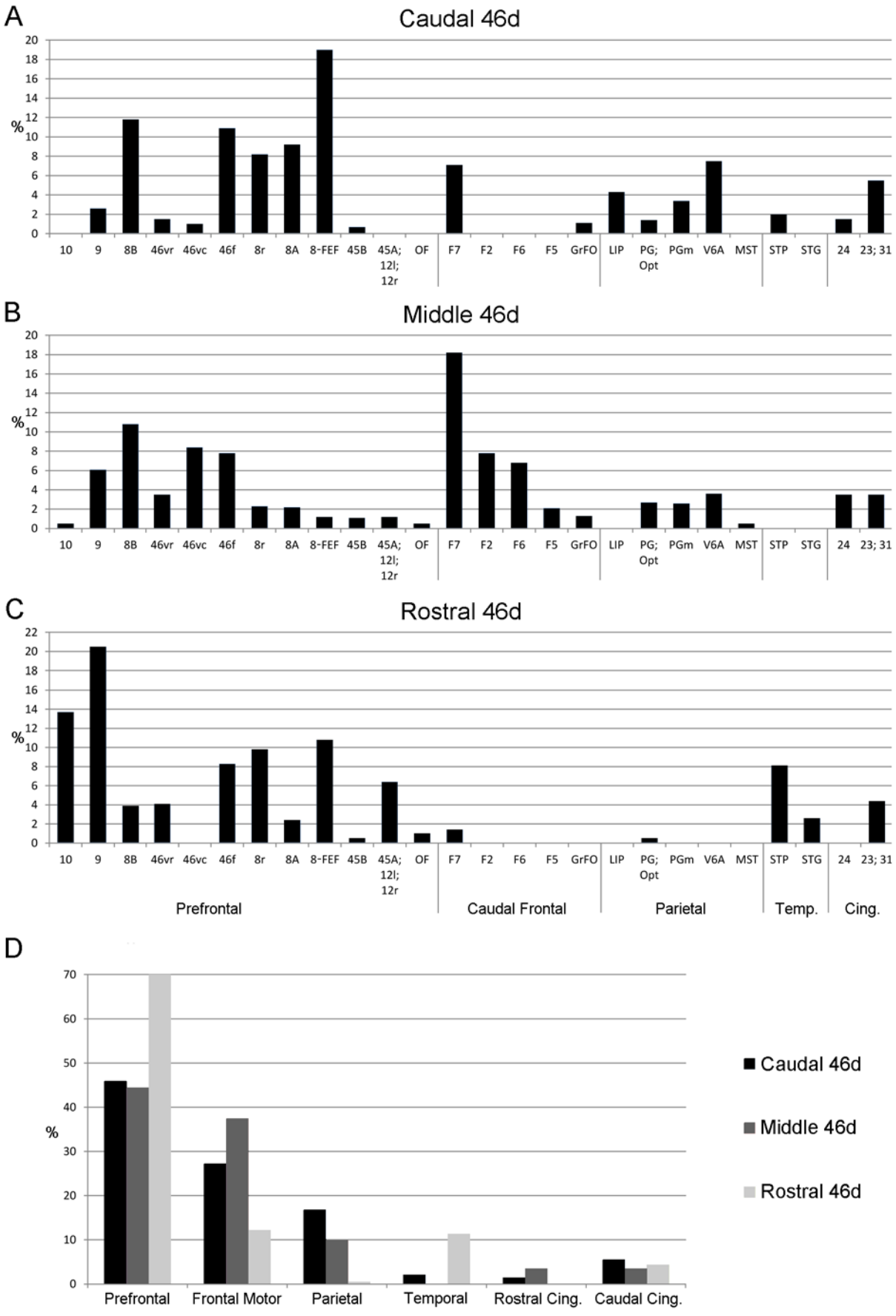
A
Caudal 46d
%
10 9 8B 46vr 46vc 46f 8r 8A 8-FEF 45B 45A; 12l; 12r OF F7 F2 F6 F5 GrFO LIP PG; Opt PGm V6A MST STP STG 24 23; 31
B
Middle 46d
%
10 9 8B 46vr 46vc 46f 8r 8A 8-FEF 45B 45A; 12l; 12r OF F7 F2 F6 F5 GrFO LIP PG; Opt PGm V6A MST STP STG 24 23; 31
C
Rostral 46d
%
10 9 8B 46vr 46vc 46f 8r 8A 8-FEF 45B 45A; 12l; 12r OF F7 F2 F6 F5 GrFO LIP PG; Opt PGm V6A MST STP STG 24 23; 31
Prefrontal
Caudal Frontal
Parietal
Temp.
Cing.
D
%
Prefrontal
Frontal Motor
Parietal
Temporal
Rostral Cing.
Caudal Cing.
Caudal 46d
Middle 46d
Rostral 46d

Figure 10

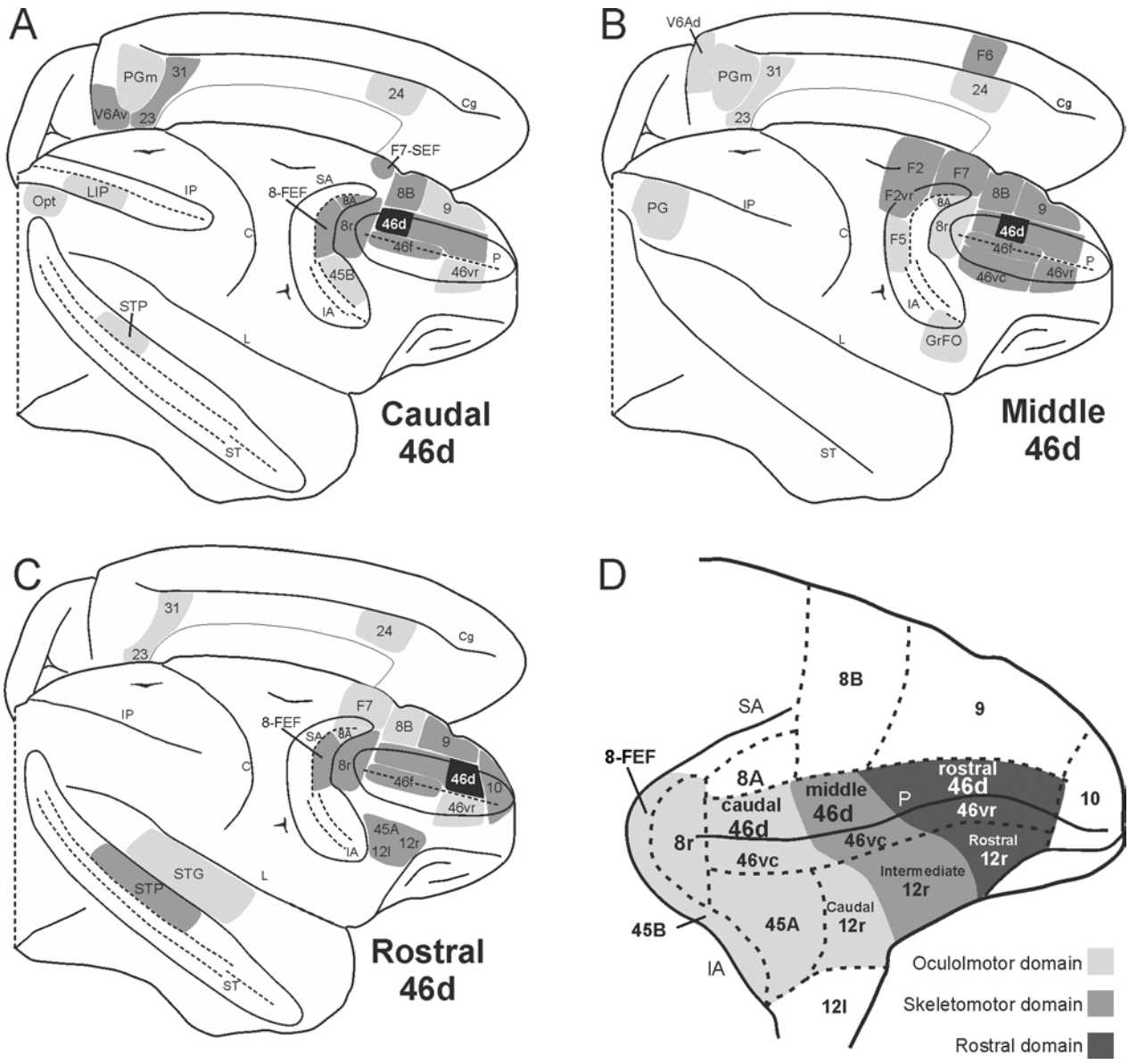
A
PGm
31
V6Av
23
24
Cg
F7-SEF
Opt
LIP
IP
8-FEF
SA
8A
8B
9
8r
46d
46f
P
46vr
45B
IA
C
L
STP
ST
Caudal
46d
B
V6Ad
PGm
31
23
F6
24
Cg
F2
F7
F2vr
8A
8B
9
PG
IP
C
8r
46d
F5
46f
P
46vc
46vr
IA
L
GrFO
ST
Middle
46d
C
31
23
24
Cg
IP
F7
8-FEF
SA
8A
8B
9
8r
46d
46f
10
46vr
C
45A
12r
IA
12l
STG
STP
L
ST
Rostral
46d
D
8B
SA
9
8-FEF
8A
rostral
46d
caudal
46d
middle
46d
P
46vr
10
8r
46vc
46vc
Rostral
12r
Intermediate
12r
Caudal
12r
45B
45A
IA
12l
Oculolmotor domain
Skeletomotor domain
Rostral domain

Figure 11

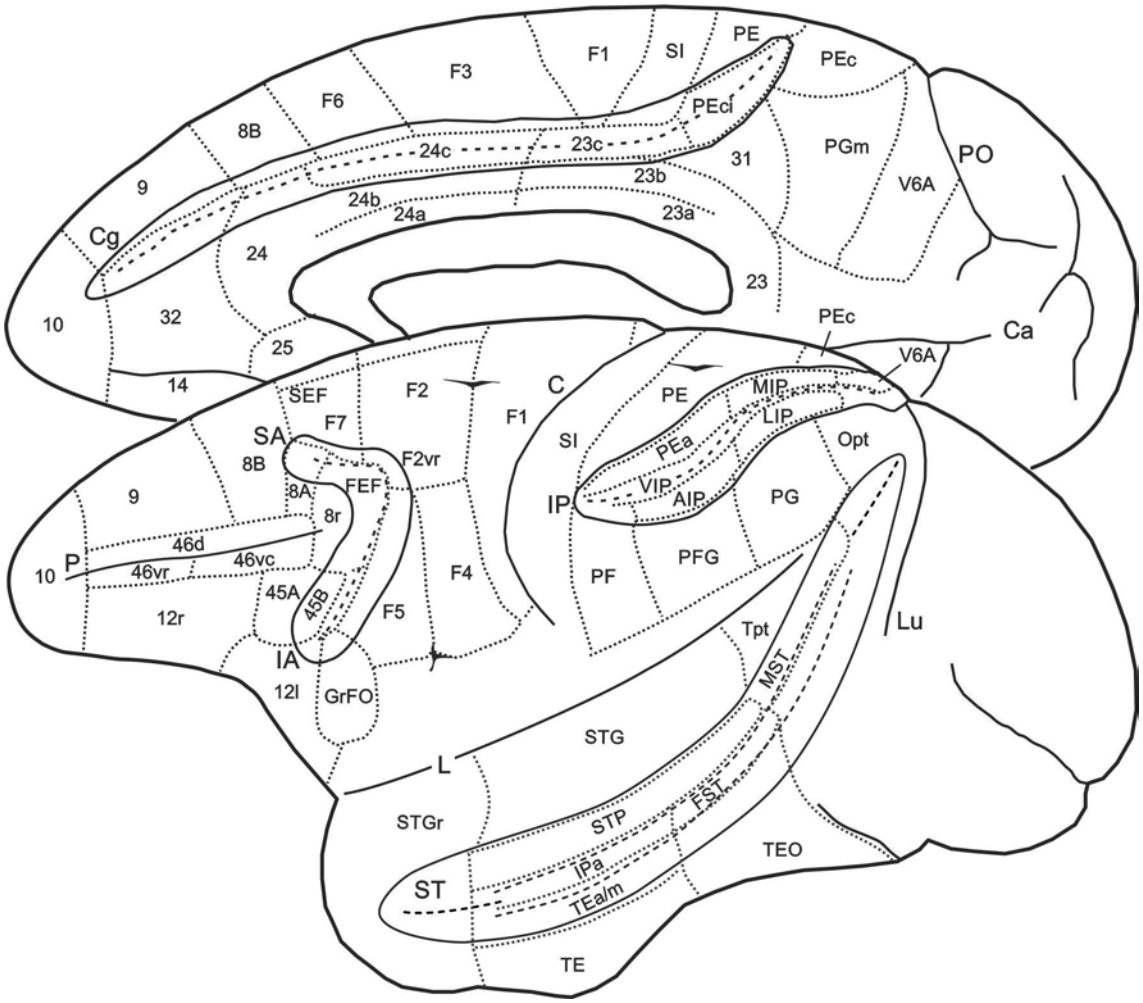

Supplementary Figure 1